

AD-A039 947

IRT CORP SAN DIEGO CALIF

F/G 20/12

EFFECTS OF LOW-TEMPERATURE NEUTRON IRRADIATION ON ARSENIC-DOPED--ETC(U)

FEB 77 A H KALMA, C J FISCHER

F19628-75-C-0138

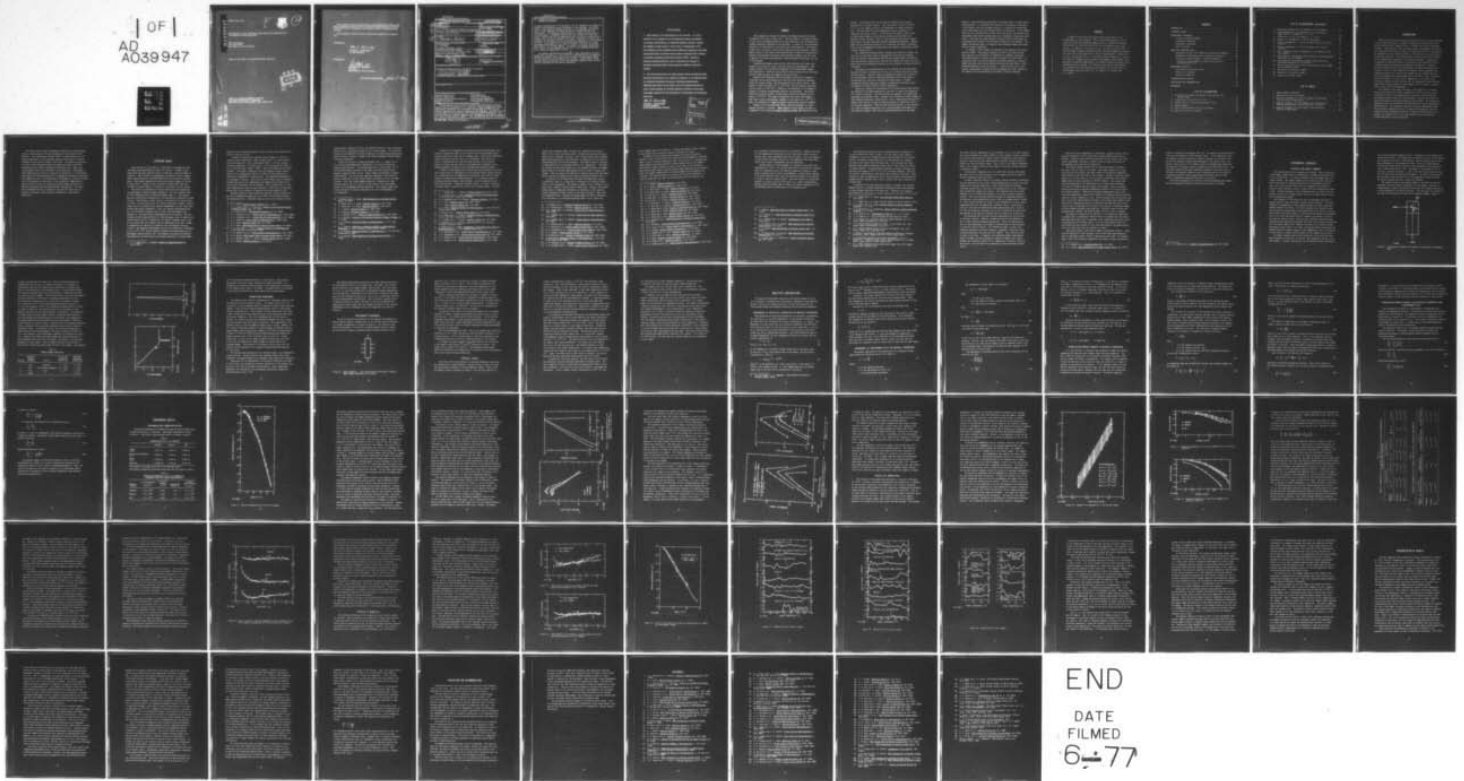
UNCLASSIFIED

INTEL-RT-8129-007

RADC-TR-77-84

NL

1 OF 1
AD
A039947



END

DATE
FILMED
6-77

AD A 039947

RADC-TR-77-84

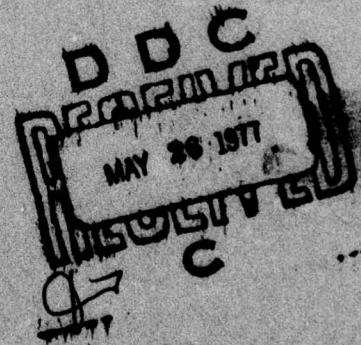


12

**EFFECTS OF LOW-TEMPERATURE NEUTRON IRRADIATION
ON ARSENIC-DOPED SILICON**

IRT Corporation
P.O. Box 80817
San Diego, California 92138

Approved for public release; distribution unlimited



ROME AIR DEVELOPMENT CENTER
AIR FORCE SYSTEMS COMMAND
GRIFFISS AIR FORCE BASE, NEW YORK 13441

AD No. _____
DDC FILE COPY

This report has been reviewed by the RADC Information Office (OI) and is releasable to the National Technical Information Service (NTIS). At NTIS it will be releasable to the General Public, including foreign nations.

This technical report has been reviewed and approved for publication.

APPROVED:

Peter J. Drevinsky
PETER J. DREVINSKY
Project Engineer

APPROVED:

Robert M. Barrett
ROBERT M. BARRETT
Director
Solid State Sciences Division

FOR THE COMMANDER:

John P. Huss

UNCLASSIFIED

SECURITY CLASSIFICATION OF THIS PAGE (When Data Entered)

REPORT DOCUMENTATION PAGE		READ INSTRUCTIONS BEFORE COMPLETING FORM	
1. REPORT NUMBER RADC-TR-77-84	2. GOVT ACCESSION NO.	3. RECIPIENT'S CATALOG NUMBER	
4. TITLE (and Subtitle) Effects of Low-Temperature Neutron Irradiation on Arsenic-Doped Silicon	5. TYPE OF REPORT & PERIOD COVERED FINAL Report 1 Apr 75 - 30 Sep 76		
7. AUTHOR(s) A. H. Kalma and C. J. Fischer	6. PERFORMING ORG. REPORT NUMBER INTEL-RT-8129-007	8. CONTRACT OR GRANT NUMBER(s) F19628-75-C-0138	
9. PERFORMING ORGANIZATION NAME AND ADDRESS IRT Corporation P.O. Box 80817 San Diego, California 92138	10. PROGRAM ELEMENT, PROJECT, TASK AREA & WORK UNIT NUMBERS 61102F 56211001		
11. CONTROLLING OFFICE NAME AND ADDRESS Deputy for Electronic Technology (RADC) Hanscom AFB, Massachusetts 01731 Monitor: Peter J. Drevinsky/ETSR	12. REPORT DATE Feb 1977	13. NUMBER OF PAGES 76	
14. MONITORING AGENCY NAME & ADDRESS (if different from Controlling Office) 12 78 p.	15. SECURITY CLASS. (of this report) Unclassified		
16. DISTRIBUTION STATEMENT (of this Report) Approved for public release, distribution unlimited. 16 5624 17 10			
17. DISTRIBUTION STATEMENT (of the abstract entered in Block 20, if different from Report)			
18. SUPPLEMENTARY NOTES			
19. KEY WORDS (Continue on reverse side if necessary and identify by block number) Arsenic-doped silicon Photoconductivity Neutron irradiation Electrical properties Long-wavelength infrared detectors Liquid-helium temperature Irradiation effects Low-background conditions			
20. ABSTRACT (Continue on reverse side if necessary and identify by block number) Arsenic-doped silicon material obtained from LWIR detector manufacturers (Aerojet and Rockwell) or a supplier of these manufacturers (High Performance Technology) was irradiated with neutrons at 10°K, and the optical response and electrical properties were measured. The material was of the grade from which quality LWIR detectors could be fabricated. The primary effect of irradiation was the net introduction of acceptor centers at a rate of approximately 16/cm ⁻¹ . This introduction rate was independent			

671A

409388 ✓

Y/B

UNCLASSIFIED

SECURITY CLASSIFICATION OF THIS PAGE(When Data Entered)

20. ABSTRACT (continued)

of oxygen concentration in the material, but its dependence on arsenic or acceptor concentration was not determined in this program. The primary effect of the radiation-induced acceptors is to compensate the arsenic levels, which decreases the majority-carrier lifetime and thus the responsivity. The acceptors also decrease the carrier concentration at low temperature. Irradiation-induced mobility changes are relatively slight, showing that the low-temperature mobility prior to irradiation is primarily set by neutral impurity scattering. Some band tailing is produced by the radiation, but this is unstable and anneals to a large extent by 100°K. It is replaced by a short-wavelength depression (or a long-wavelength enhancement) in the spectral response, which may be another manifestation of the same defects. In general, the damage effects were quite stable, and few changes were observed in the measured properties up to annealing temperatures of 400°C.

The damage concentration introduced in these experiments was small enough that, in general, it only acted as a perturbation on the measured material properties, which were still set mainly by the arsenic dopant. To study the nature of the defects more carefully, higher defect concentrations would be required so that the measured properties would be more directly determined by the defects themselves.

UNCLASSIFIED

SECURITY CLASSIFICATION OF THIS PAGE(When Data Entered)

EVALUATION

1. This report is the Final Report on the contract. It covers research on the effects of low-temperature neutron irradiation on arsenic-doped silicon, an infrared detector material, during the eighteen-month period 1 April 1975 to 30 September 1976. The objective of this research was to determine changes in impurity photoconductivity of arsenic-doped silicon irradiated with neutrons at detector operating temperatures (below 20°K), determine thermal annealing behavior, and to correlate the changes in impurity photoconductivity with prominent radiation-produced defects.

2. The work performed is of value because it has provided the first extensive information on the effects of neutrons on an infrared detector material irradiated at detector operating temperatures. Although information on the nature of the irradiation-induced defects is still lacking, the results obtained contribute to the basic knowledge required for the development of techniques for hardening detectors.

Peter J. Drevinsky
PETER J. DREVINSKY
Project Engineer
Solid State Sciences Division

ACQUISITION FOR	
DTIC	White Section <input checked="" type="checkbox"/>
DDC	Diff Section <input type="checkbox"/>
UNANNOUNCED	<input type="checkbox"/>
JUSTIFICATION	<input type="checkbox"/>
BY	
DISTRIBUTION/AVAILABILITY CODES	
Dist.	AVAIL. AND/OR SPECIAL
A	

SUMMARY

This program was designed to examine the damage produced by neutron irradiation of silicon at about 10°K. This knowledge is necessary because it will allow the damage mechanisms in LWIR detectors to be determined and perhaps hardening techniques to be developed. In order for the information obtained to be applicable to state-of-the-art LWIR detectors, the material studied must be similar to that used to fabricate such detectors. Arsenic-doped silicon of this quality was obtained from two detector manufacturers, Rockwell International and Aerojet ElectroSystems Company, and also from a supplier of detector manufacturers, High Performance Technology, for use in the program.

Standard measurement conditions for LWIR detectors were taken into account and achieved as much as possible during the measurements. This primarily meant that the optical background in the measurement chamber was significantly reduced by using field-of-view limiting and by filtering external light entering the chamber with cold filters.

Samples were fabricated from the different materials by standard techniques and the photoconductivity and electrical properties measured. Except for oxygen content, the three materials were quite similar. Their arsenic content was about 2 to 3 x 10¹⁶ cm⁻³, and the acceptor concentration was about 6 x 10¹³ cm⁻³. Therefore, the dependence of the damage on arsenic or acceptor concentration could not be determined. The Aerojet material was pulled crystal, so the oxygen content was probably on the order of 10¹⁸ cm⁻³. The other two materials were float zone refined with lower oxygen concentration, probably on the order of 5 x 10¹⁶ cm⁻³. Thus, the dependence of damage on oxygen concentration could be examined.

Samples were irradiated with fission neutrons produced by a photo-nuclear reaction in fansteel. Gamma exposure of the samples was kept to a minimum by using depleted uranium shielding between the fansteel and the

samples. The primary effect of the neutron irradiation was the net introduction of acceptor centers. This occurred at a rate of about 16 cm^{-1} in all the samples and thus was independent of oxygen concentration. The main effect of these irradiation-induced acceptors is to compensate the arsenic levels. This produces more empty arsenic sites at which excited majority carriers can recombine and decreases the majority-carrier lifetime. This, in turn, decreases the optical responsivity and is the most important detector degradation mechanism. Another effect of the additional acceptors is to decrease the carrier concentration in the low temperature region where the acceptor concentration exerts a direct control on it.

The irradiation-induced mobility changes were relatively slight, and thus were not the major cause of degradation of the optical response. Since the acceptor concentration and thus the charged-impurity concentration approximately doubled while the mobility changed only about 10%, this means that the preirradiation mobility was set primarily by neutral-impurity scattering.

The nature of the defects that act as acceptors was not determined because the defect concentration was too low to observe any direct effect from the defects. The only means of studying the defects was indirectly by observing their effect on measured properties such as the impurity photoconductivity that were controlled by other things. A higher irradiation fluence producing a greater concentration of defects would be required to better study the defects themselves.

There was evidence of the production of disorder because band tailing was observed in the photoconductivity, and this is usually considered to be a result of disorder. The band tailing was unstable, and significant annealing occurred below 100°K . However, the irradiation-induced changes in other measured properties showed little, if any, comparable annealing so it appears that whatever caused the band tailing had no significant effect on the other properties. When the band tailing annealed, it was replaced by a short-wavelength depression (or a long-wavelength enhancement) of the spectral response, which may be another manifestation of the same

defects. Since the band tailing seems to be more stable at higher defect concentrations, it is possible that overlap of the regions of influence of the defects, which are perhaps clusters, is required for photoconductivity enhancement near the intrinsic band to be produced. If the defects have too low a concentration so that no overlap occurs, photoconductivity enhancement would not be produced and only a competitive absorption would result. There was also some evidence of shallow levels which might be associated with disorder in the electrical properties measurements. The number involved was small, so equating other measured changes with these levels is open to question.

In general, little change was observed in any property with annealing up to 400°C. The obvious exception to this is the band tailing. This stability of the effects of irradiation is somewhat surprising, since many defects in silicon are known to anneal well below 400°C. It is possible that all of this previously observed annealing is actually defect evolution, and the new defects have much the same effect on the measured properties as the old defects. It would not be until a sufficient concentration of defects were introduced that direct effects of the defects could be observed and the defect evolution examined.

PREFACE

A number of individuals and organizations contributed to the accomplishment of this program. IRT is particularly grateful to C. M. Parry of Aerojet ElectroSystems Company and R. A. Florence of Rockwell International for supplying some of the silicon material used in the testing. In addition, we are grateful to F. M. Hoke of the Ballistic Missile Defense Advanced Technology Center, on whose programs the material was grown, for giving permission to the two organizations to supply the silicon. Discussions with P. J. Drevinsky (contract monitor), J. Silverman, and H. M. DeAngelis of the Rome Air Development Center [Deputy for Electronic Technology (RADC/ETSR)], also greatly aided the authors in the performance of the program. In addition to the effort of the authors, the contribution to the program of other members of the IRT staff is acknowledged, especially that of R. A. Cesena, R. E. Leadon, and C. E. Mallon.

(CONTINUED) LIST OF ILLUSTRATIONS

CONTENTS

INTRODUCTION	1
LITERATURE SURVEY	3
EXPERIMENTAL TECHNIQUES	14
Cryostat and Sample Chamber	14
Irradiation Procedures	18
Measurement Procedures	19
Material Tested	20
ANALYTICAL CONSIDERATIONS	23
Dependence of Electrical Properties on Material Parameters	23
Dependence of Photoconductivity on Material Parameters	24
Irradiation-Induced Changes in Material Parameters	26
Irradiation-Induced Changes in Electrical Properties and Photoconductivity	29
EXPERIMENTAL RESULTS	31
Preirradiation Characterization	31
Effects of Irradiation	38
Effects of Annealing	47
INTERPRETATION OF RESULTS	57
CONCLUSIONS AND RECOMMENDATIONS	62
REFERENCES	64

LIST OF ILLUSTRATIONS

1. Orientation of sample with respect to the optical and magnetic axes	15
2. Transmission of the Al-on-Si filter	17
3. Transmission of 4.1- μ m narrow-bandpass filter	17
4. Sample geometry	19
5. Carrier concentration of the Si:As samples	32
6. Mobility of the Si:As samples	35

LIST OF ILLUSTRATIONS (CONTINUED)

7. Wavelength dependence of the response of Si:As samples	35
8. Length dependence of the responsivity of the Autonetics sample prior to irradiation, $\lambda = 4.1 \mu\text{m}$	37
9. Responsivity of the Si:As samples, $\lambda = 4.1 \mu\text{m}$	37
10. Responsivity degradation in the Aerojet sample	40
11. Response degradation in the Si:As samples with no intrinsic injection.	41
12. Response degradation in the Si:As samples with intrinsic injection.	41
13. Post-irradiation spectral dependence of the response of the Si:As samples.	46
14. 100°K anneal of the Aerojet sample showing the long-wavelength enhancement of the response.	49
15. 175°K anneal of the Autonetics sample showing the short-wavelength depression of the response.	49
16. Shift of the slope of the carrier concentration versus 1000/T for the Rockwell sample.	50
17. Annealing of the Rockwell sample	51
18. Annealing of the Aerojet sample.	52
19. Annealing of the HPT sample.	53

LIST OF TABLES

1. Sample Chamber Conditions	16
2. Dimensions of the Si:As Samples	31
3. Materials Parameters of the Si:As Samples as Determined from the Carrier Concentration.	31
4. Material Parameters of Si:As Samples from the Electrical Properties Measurements Before and After Irradiation.	43
5. Material Parameters of Si:As Samples from the Optical Properties Measurements	43

INTRODUCTION

Doped silicon detectors are being increasingly used as long-wavelength infrared (LWIR) detectors. A number of impurities have been used, with arsenic being the most common because it produces the desired wavelength response. LWIR detectors could encounter nuclear environments; therefore, it is important that the basic physics of radiation effects in the material be understood so that radiation effects in the detectors can be predicted and perhaps minimized. Since LWIR detectors operate below $\sim 20^\circ\text{K}$, studies in this temperature regime are of particular importance. Considerable information on radiation effects is available in the literature, with a reasonable amount concerning low-temperature irradiations. However, neutron-irradiation data at low temperatures is almost completely nonexistent. This is a very important environment, because neutrons are a significant portion of a nuclear environment and are probably the part of the environment that would damage silicon the most. Thus, information on neutron damage in silicon at low temperatures is necessary, with particular emphasis on those effects that are important to LWIR detectors. Specifically, photoconductivity measurements on Si:As doped to an appropriate level need to be emphasized.

The purpose of the study described in this report was to examine directly the effects of neutron irradiation at 10°K on silicon so that information to fill this important gap in the data could be obtained. The damage processes that occur and the manner in which they affect the material parameters and device properties were studied. The program was designed so that the information obtained would be directly applicable to LWIR detectors. The mechanisms involved in detector degradation would thus be better understood so that (1) detector vulnerability could be predicted from a knowledge of detector or material characteristics, and perhaps (2) information on how to make detectors less vulnerable to neutron degradation could be obtained.

The scope of this effort encompassed irradiation of arsenic-doped silicon with neutrons at 10°K and examination of the effects on the material. The relationship of these effects to LWIR detectors was of primary importance, so the study was tailored specifically to provide information that would be useful in this area. The material tested was as close to that from which quality detectors are made as possible. Examination of the effect of material differences (e.g., float zone versus pulled crystal) was also part of the study task. The measurements emphasized were those of importance to detectors, so the principal measurement was the photoconductivity, although the electrical properties were examined as well. The annealing of the damage, at least up to 300°K, was to be examined (in some cases it was examined at temperatures as high as 400°C) as an aid in characterizing the damage and also as a potential mechanism for lessening detector vulnerability. The information obtained from these studies was analyzed for application to detector technology so that detector vulnerability can be better understood.

LITERATURE SURVEY

Over the past 15 to 20 years, a large body of knowledge has been developed concerning radiation effects in silicon. A number of the areas which have been explored relate in some way to neutron damage in detectors. These include low-temperature irradiation, neutron damage, defect characterization, and photoconductivity and electrical measurements. One largely unexplored area has been neutron damage in silicon at about 10°K. A review of the literature in these areas and their relation to neutron effects in detectors is discussed in this section.

Most neutron irradiations of silicon done below room temperature are performed at liquid-nitrogen temperature. The only reported study at lower temperature was by Cheng and Swanson (Ref. 1). The measurement tool used was photoconductivity, and the material studied was p-type silicon. Arsenic-doped silicon, which is the material of interest here, is n-type, so these results are not directly applicable; however, neutron effects are to a certain extent impurity-independent, so this study does provide some useful information. Also, the impurity photoconductivity was not specifically observed, and, in fact, the measurements were designed so that only defect photoconductivity was observed. The conclusions of this study were that (1) neutron damage occurs in defect-rich clusters which are still crystalline, (2) shallow trapping levels close to the valence band are produced, and (3) annealing occurs over a range of temperatures by emission of vacancies and interstitials from the clusters. The impurity photoconductivity was not affected by irradiation to 3.6×10^{12} n/cm², and the defects increased the photoconductivity at wavelengths short of about 5 μ m. The findings concerning the physical characteristics of the cluster are probably applicable to arsenic-doped

-
1. L. J. Cheng and M. L. Swanson, Journal of Applied Physics **41**, 2627 (1970).

material, but the defect properties such as energy levels and photoconductivity spectra are not.

A number of studies have examined neutron damage in silicon at liquid-nitrogen temperature. Some of these (Refs. 2,3) have examined the photoconductivity, and a large number (Refs. 4-10) have studied electrical properties. Lifetime (Refs. 11-13) and absorption (Refs. 10, 12,14) have also been studied. Both n- and p-type materials have been examined. The primary finding was that the neutrons produce cluster defects at all temperatures from 78 to 300°K, and the production is essentially independent of material type. The temperature-dependence of the damage is unclear. Electrically active defects show a decreased introduction rate at low temperature, but damage in the center of the cluster may be shielded and not measured. Thus, extrapolation to even lower temperatures cannot be done accurately. This is one of the prime reasons why it was essential to measure the neutron damage at 10°K.

Another finding of these studies was that the clusters anneal over the entire temperature range from 78 to 300°K, and illumination makes the annealing faster. Individual defects such as the divacancy and the

-
2. H. J. Stein, Applied Physics Letters **15**, 61 (1969).
 3. V. S. Vavilov and A. F. Plotnikov, Journal of the Physical Society of Japan **18 Suppl. III**, 230 (1962).
 4. C. D. Clark et al., Philosophical Magazine **20**, 301 (1969).
 5. K. L. Starostin et al., Soviet Physics--Semiconductors **1**, 1520 (1968).
 6. K. L. Starostin et al., Soviet Physics--Semiconductors **2**, 505 (1968).
 7. K. L. Starostin, Soviet Physics--Semiconductors **4**, 1569 (1971).
 8. H. J. Stein, Physical Review **163**, 801 (1967).
 9. H. J. Stein, IEEE Transactions on Nuclear Science **NS-15**, 69 (1968).
 10. F. L. Vook and H. J. Stein, Radiation Effects in Semiconductors, p. 99, New York: Plenum Press (1968).
 11. V. N. Alfas'ev et al., Soviet Physics--Semiconductors **5**, 1967 (1971).
 12. C. E. Barnes, IEEE Transactions on Nuclear Science **NS-16**, 28 (1969).
 13. H. T. Henderson and K. L. Ashley, Physical Review **186**, 811 (1969).
 14. C. E. Barnes, Radiation Effects **8**, 221 (1971).

oxygen-vacancy complex (A-center) are produced directly by the irradiation and also their concentration grows as the clusters anneal. The individual defects can be observed by various techniques, including photoconductivity, where increased response is found in the short-wavelength infrared (SWIR) following irradiation.

Except for the work of Cheng and Swanson (Ref. 1), almost all of the liquid-helium-temperature irradiations in silicon have been performed using electrons. A few photoconductivity studies (Refs. 15-17) have been performed, and most of the others utilized electron paramagnetic resonance (Refs. 18-25). These studies concentrated on defect identification. One of the most important findings is that intrinsic defects--especially silicon interstitials--are mobile at very low temperatures. Thus, the stable damage produced by irradiation at temperatures even as low as 4.2°K will be the result of both the damage process and rearrangement through annealing. This probably means that clusters produced by neutron irradiation will show rearrangement at low temperature.

15. M. Cherki and A. H. Kalma, IEEE Transactions on Nuclear Science NS-16, 24 (1969).
16. M. Cherki and A. H. Kalma, Physical Review B 1, 647 (1970).
17. P. Vajda and L. H. Cheng, Radiation Effects 8, 245 (1971).
18. K. L. Brower, Physical Review B 1, 1908 (1970).
19. B. Goldstein, Radiation Effects 8, 229 (1971).
20. G. D. Watkins et al., Journal of Applied Physics 30, 1198 (1959).
21. G. D. Watkins, Journal of the Physical Society of Japan 18 Suppl. II, 22 (1963).
22. G. D. Watkins, Radiation Damage in Semiconductors, p. 97, Dunod (1965).
23. G. D. Watkins, Symposium on Radiation Effects in Semiconductor Components, p. A1-9, Journées d'Electronique (1968).
24. G. D. Watkins, Radiation Effects in Semiconductors, p. 97, New York: Plenum Press (1968).
25. G. D. Watkins, IEEE Transactions on Nuclear Science NS-16, 13 (1969).

A number of low-temperature irradiations have been performed using electrical properties (Refs. 26-28), and one has been performed using thermal conductivity (Ref. 29) as a damage probe. Since these properties require heating to provide their full information, they are not as useful as photoconductivity and EPR where heating is not required. However, evidence has been found of low-temperature annealing such as damage-dependence on impurity and low-temperature annealing stages.

A number of photoconductivity studies have been performed in silicon. Since a great deal of information can be obtained without sample heating, it is often used for low-temperature irradiations; thus, many of these studies are among those already mentioned. It is also more useful in studying individual defects than disorder, so most irradiations have been with electrons. Cheng and co-workers (Ref. 1,17,30,31), Kalma and co-workers (Refs. 15,16,32-36), Vavilov and co-workers (Refs. 3,37-40),

26. P. S. Gwozdz and J. S. Koehler, Physical Review B **6**, 4571 (1973).
27. E. E. Klontz and L. L. Sivo, Radiation Effects in Semiconductors, p. 136, New York: Plenum Press (1968).
28. R. E. McKeighen and J. S. Koehler, Radiation Effects **9**, 59 (1971).
29. F. L. Vook, Physical Review **138**, A1234 (1965).
30. L. J. Cheng, Physics Letters **24A**, 729 (1967).
31. L. J. Cheng, Radiation Effects in Semiconductors, p. 143, New York: Plenum Press (1968).
32. M. Caillot et al., Physica Status Solidi A **4**, 121 (1971).
33. A. H. Kalma and J. C. Corelli, Radiation Effects in Semiconductors, p. 153, New York: Plenum Press (1968).
34. A. H. Kalma and J. C. Corelli, Physical Review **173**, 734 (1968).
35. B. Goldstein et al., Colloque International sur les Cellules Solaires, Toulouse (1970).
36. M. Cherki and A. H. Kalma, Proceedings of the Third Intl. Conf. on Photoconductivity, p. 279, Pergamon Press (1971).
37. I. P. Akimchenko et al., Soviet Physics--Semiconductors **3**, 132 (1969).
38. I. P. Akimchenko et al., Soviet Physics--Solid State **10**, 3677 (1964).
39. V. D. Tkachev et al., Soviet Physics--Solid State **5**, 1332 (1964).
40. V. D. Tkachev et al., Soviet Physics--Solid State **5**, 2333 (1964).

Corelli and co-workers (Refs. 33,34,41,42), Tkachev and co-workers (Refs. 43-47), and a few others (Refs. 2,48,49) have studied the photoconductivity of defects in silicon. All of these efforts have examined defect photoconductivity, and the effect of irradiation on the impurity photoconductivity has not been examined. The defects cause an increase in photoconductivity in the SWIR region at all temperatures. The effect of disorder on the photoconductivity is an apparent decrease in bandgap, which causes the intrinsic photoconductivity to extend to longer wavelengths. This is possibly the addition of shallow states near the bands, which could be the trapping levels found by Cheng and Swanson (Ref. 1).

In addition to the previously discussed low-temperature neutron irradiations, there is a large body of information on neutron irradiations at room temperature. The number of papers in the literature is so great that a complete listing would be quite long. However, the primary finding which is important for defects in detectors is that neutrons produce disordered clusters, which is the same conclusion drawn from low-temperature work. The most striking example of efforts leading to this conclusion is in electron microscopy (Refs. 50-53), where the

-
41. E. Fenimore et al., Journal of Applied Physics 43, 1962 (1972).
 42. R. C. Young and J. C. Corelli, Physical Review B 5, 1455 (1972).
 43. M. T. Lappo and V. D. Tkachev, Soviet Physics--Semiconductors 4, 1882 (1970).
 44. P. F. Lugakov and V. D. Tkachev, Soviet Physics--Semiconductors 1, 295 (1967).
 45. P. F. Lugakov and V. D. Tkachev, Soviet Physics--Semiconductors 1, 569 (1967).
 46. V. D. Tkachev and M. T. Lappo, Radiation Effects 9, 81 (1971).
 47. V. S. Vavilov et al., Soviet Physics--Solid State 4, 2522 (1965).
 48. A. B. Gerasimov et al., Soviet Physics--Solid State 8, 2390 (1967).
 49. M. L. Swanson, Physica Status Solidi 33, 721 (1969).
 50. M. Bertolotti et al., Journal of Applied Physics 38, 2645 (1967).
 51. M. Bertolotti, Radiation Effects in Semiconductors, p. 311, New York:Plenum Press (1968).
 52. J. M. Pankratz et al., Journal of Applied Physics 39, 101 (1968).
 53. J. M. Pankratz and N. L. Rudee, Physica Status Solidi 26, K97 (1968).

actual damage regions are observed. In these experiments, direct evidence of the production of localized regions of disorder was found.

A number of other studies have examined the defects produced by neutrons. Most of these studies have used electron paramagnetic resonance (Refs. 54-60) or optical properties (Refs. 30,31,46,61-75). Although some simple defects have been observed in these studies, most of the defects observed were complex defects at least on the order of the divacancy. Many of the simple defects observed evolved upon annealing of the clusters. Thus, the primary characteristic of neutron damage is the formation of clusters. The characteristics of clusters are not well understood. A study by Cheng and Lori (Ref. 65) has indicated that the clusters are

54. K. L. Brower, Radiation Effects **8**, 213 (1971).
55. K. L. Brower, Physical Review B **4**, 1968 (1971).
56. D. F. Daly and H. E. Nofke, Radiation Effects **8**, 203 (1971).
57. D. F. Daly and H. E. Nofke, Radiation Effects **10**, 191 (1971).
58. W. Jung and G. S. Newell, Physical Review **132**, 648 (1963).
59. Y-H Lee and J. W. Corbett, Physical Review B **9**, 4351 (1974).
60. Y-H Lee and J. W. Corbett, Physical Review B **8**, 2810 (1973).
61. C. S. Chen and J. C. Corelli, Radiation Effects **9**, 75 (1971).
62. C. S. Chen and J. C. Corelli, Physical Review B **3**, 1505 (1972).
63. L. J. Cheng and P. Vajda, Journal of Applied Physics **40**, 4679 (1969).
64. L. J. Cheng and P. Vajda, Physical Review **186**, 816 (1969).
65. L. H. Cheng and J. Lori, Physical Review **171**, 856 (1968).
66. L. J. Cheng and J. Lori, Applied Physics Letters **16**, 324 (1970).
67. J. C. Corelli et al., IEEE Transactions on Nuclear Science **NS-17**, 128 (1970).
68. T. D. Dzhafarov, Soviet Physics--Semiconductors **5**, 697 (1971).
69. Yu. P. Koval' et al., Soviet Physics--Semiconductors **5**, 2061 (1972).
70. E. N. Lotkova, Soviet Physics--Solid State **6**, 1224 (1964).
71. A. K. Ramdas and M. G. Rao, Physical Review **142**, 451 (1966).
72. F. L. Vook and H. J. Stein, Radiation Effects **2**, 23 (1969).
73. R. E. Whan, Journal of Applied Physics **37**, 3378 (1966).
74. J. A. Naber et al., Radiation Effects **8**, 239 (1971).
75. V. N. Mordkovich et al., Soviet Physics--Semiconductors **6**, 1643 (1973).

still primarily crystalline and rich in divacancies. Whether this held for low-temperature irradiations or the relatively ordered structure evolved from a more disordered state was not known. Also, the number of isolated defects produced directly at low temperature and those which result from cluster rearrangement must be determined.

Another aspect of neutron damage is a feature called short-term annealing (Ref. 76-81). On a short time scale (microseconds to seconds) after an irradiation pulse, the material properties recover to some extent, probably due to cluster rearrangement. Vacancy motion appears to be quite important here, since the activation energy of the process is close to that for vacancy motion. Since the vacancy is essentially immobile in n-type silicon at 10°K (Ref. 21), cluster reorganization probably would be nowhere near as large as at higher temperatures, and the disorder would be present more in its original state.

-
76. I. Arimura, IEEE Transactions on Nuclear Science NS-17, 348 (1970).
 77. O. L. Curtis Jr., IEEE Transactions on Nuclear Science NS-17, 105 (1970).
 78. B. L. Gregory and H. H. Sander, Proceedings of the IEEE 58, 1328 (1970).
 79. J. W. Harrity and C. E. Mallon, IEEE Transactions on Nuclear Science NS-17, 100 (1970).
 80. R. E. Leadon, IEEE Transactions on Nuclear Science NS-17, 110 (1970).
 - 80a. C. E. Mallon and J. W. Harrity, IEEE Transactions on Nuclear Science NS-18, 45 (1971).
 81. J. R. Srour and O. L. Curtis Jr., Journal of Applied Physics 40, 4082 (1969).

Some additional data does exist concerning neutron irradiation of silicon at about 10°K (Refs. 82-93); it is not exactly basic physics information, since such irradiations have been performed on IR detectors. However, the impurity photoconductivity of the material was examined, and some of the results have relevance here. The detectors have been measured under reduced background because that is the condition in which IR sensors operate. Silicon doped with arsenic, antimony, bismuth, and gallium in the range of 10^{15} to 10^{17} cm⁻³, has been examined. These are the impurity concentrations from which quality detectors are made. Other impurities, such as compensation levels, had the proper concentration for optimum carrier lifetime; hence, that is exactly the type of material of interest here.

In general, the n-type impurities (arsenic, antimony, and bismuth) behaved similarly, although significant differences often were observed at times between detectors of the same type. Generally, the impurity photoconductivity decreases at neutron fluences on the order of 10^{13} n/cm².

82. J. A. Naber and A. H. Kalma, 10th Midcourse Measurements Meeting, 251 (1971).
83. J. A. Naber and A. H. Kalma, Nuclear Effects on Optics Seminar (1971).
84. J. A. Naber and A. H. Kalma, Nuclear Effects on Optics Technical Briefing, 1.7.1 (1972).
85. A. H. Kalma and B. C. Passenheim, Nuclear Effects on Optics Technical Briefing, 3.3.1 (1972).
86. A. H. Kalma et al., Proceedings on IRIS 18, No. 2, 137 (1973).
87. A. H. Kalma et al., Joint Strategic Sciences Meeting (1974).
88. A. H. Kalma et al., "Detector Radiation Damage Effects, Vol. IV," report number MS-ABMDA-1697 (May 1973).
89. A. H. Kalma, "Detector Radiation Damage Effects Study, Vol. III," report number DNC74EG566581 (July 1974).
90. A. H. Kalma, "Hardened Detector/Circuit Development, Vol. III," report number 5059 (September 1974).
91. M. Warren, "Investigation of Nuclear Radiation Effects on Infrared Detectors", report number AFCRL-TR-73-0346 (August 1973).
92. R. A. Florence, "Hardened Focal Plane Development", Vol. I, Appendix A, "Permanent Damage Nuclear Effects Study", A. H. Kalma, report number DASG-75-C-0044 (August 1974).
93. A. H. Kalma, "Hardened Detectors/Circuits Study, Vol. III", report number 5254 (October 1976).

The actual spectral dependence was not measured, so it is not known whether the levels producing the signal changed or only a general decrease occurred. Less heavily doped detectors showed a faster degradation, which might be expected, since more heavily doped material requires a higher fluence to produce the same percentage change. This is not a true impurity-dependent effect; it is simply a matter of the number of intrinsic defects required to produce an effect.

In some cases, degradation was at a much lower fluence than normal. The cause of this was not uncovered, and it remains one of the areas in which a significant question exists.

At times, detectors showed an increased response following irradiation. This was observed for the p-type, gallium-doped material as well as n-type samples with different impurities. Many of those detectors showing increased response had a relatively low response prior to the irradiation which caused the response to increase. This characteristic was either inherent in the as-fabricated detectors or caused by previous radiation testing. Thus, the radiation-induced increase was changing something in the detectors and bringing them closer to what an optimum detector should be. This could have been the result of the introduction of levels which compensated initially uncompensated, shallower levels. Another possibility is that only the shorter-wavelength photoconductivity, which is all that was measured, increased, due to the introduction of deep levels. Measurement of the spectral response would be required to answer this.

The annealing done in these detector experiments was not detailed, so not much is known. Generally, annealing reversed any degradation, but at times annealing produced degradation. Since the annealing was only to room temperature, any change it produced must be the annealing of radiation-induced defects. One interesting aspect is that, when annealing degraded the detector response, subsequent irradiation often reversed the process and increased the response. This could be cycled at least a few times. It appears that annealing produces some defect which is harmful and that subsequent irradiation negates this effect. Perhaps the irradiation effect is the compensation of shallow levels by deep levels, with the deep levels annealing to form additional shallow levels.

When all of this information is correlated, a general picture of how neutron irradiation at 10°K would affect arsenic-doped silicon can be obtained. There are many questions remaining, but an overall view, even though incompletely defined, is useful to have so that the results of this program can be more easily understood.

The primary damage produced will be clustered regions of defects, but their state of order is not known. Some simple defects may be produced outside the clusters, but their effect on the material properties would likely be less than that of the clusters. However, relatively simple defects in a cluster which is still basically crystalline could produce damage that has some properties of isolated defects. The clusters may show some annealing at low temperature via an interstitial mechanism, but they will probably be quite stable until heated. Thus, the damage should be essentially impurity-independent because it will be the result of intrinsic defects. Annealing at elevated temperatures should occur over broad temperature ranges by the emission of vacancies and interstitials from the cluster, reducing its size. These vacancies and interstitials, however, could form simple defects external to the cluster which might be more effective in changing the material properties than when they were in the cluster, due to screening of the center of the cluster, so measured damage could be greater following some annealing. Injection could increase the annealing rate; however, the effectiveness of this at 10°K is unknown.

The effect of clusters on the material is not completely understood. It appears that a continuum of shallow levels is produced near both bands. Some deep levels must also be produced, since irradiation eventually drives the material to an intrinsic state. It is not known whether these are associated with the clusters or with individual defects, although association of at least some with the clusters is likely.

The shallow levels could cause a number of measurable effects. Light could be absorbed at lower energies, and the band edge would apparently shift in absorption (Refs. 94,95) or photoconductivity (Ref. 34) measurements. Also, the electrical properties could show a shallow continuum of

94. L. J. Cheng et al., Physical Review **152**, 761 (1966).

95. A. H. Kalma, IEEE Transactions on Nuclear Science **NS-20**, 224 (1973).

levels, as observed in germanium (Ref. 96). The impurity photoconductivity could also be affected by these shallow levels. If the temperature were low enough to produce essentially complete freezeout on the donor levels, but not low enough to produce much freezeout on any shallow levels, the shallow levels would act in a manner similar to uncompensated impurities and decrease the majority-carrier lifetime and the photoconductivity. The increased response following irradiation observed in detectors with an initially low response caused by prior irradiation may be the result of irradiation-produced levels compensating the shallow levels in some manner, although the mechanism involved is not obvious.

With this background, the questions that need answering are clearer, and the information obtained in this study can be put in context.

96. A. H. Kalma et al., Journal of Applied Physics **37**, 3913 (1966).

EXPERIMENTAL TECHNIQUES

CRYOSTAT AND SAMPLE CHAMBER

The cryostat used on this program was a Cryotip. This is basically a cold sample chamber which is connected to a cryogen storage dewar by a 6-foot transfer tube. It is more convenient than an upright dewar for several reasons. The sample chamber end is relatively small and can be easily moved from an irradiation position to a measurement position. Also, the 6-foot transfer tube allows the cryogens to be placed at a distance from irradiation sources to keep them from accumulating as high a dose. Another advantage is that turnaround time is quicker, and less cryogen is wasted in a warmup because there is no large reservoir which must be emptied and warmed.

The drawbacks of the Cryotip are that the available cold area is limited and that long, continuous cooling is more difficult. The first drawback was unimportant to this program because only small individual samples needed to be cooled. The latter drawback was a potential problem because the storage dewars used contained 25 or 30 liters of liquid helium, which was used at about 1.5 liters per hour during the experiments. With a few liters used during initial cooldown, the maximum continuous run time was about 15 hours. This was only a potential problem during irradiation and annealing experiments that took over 24 hours and required that the sample remain cold. However, even here, the 15 hours allowed annealing to above 150°K in all cases, and storage dewars could easily be changed before the samples heated to this temperature, even if the helium ran out during a cooldown from an anneal and the chamber was not cold.

The sample chamber used for the testing had to allow for low background operation and optical, electrical, and irradiation testing in the same chamber. Cryostat construction was of aluminum as much as possible

to cut down on neutron-induced activity. Blueprints of the chamber were submitted previously. The chamber has an optical axis that is end-looking and a magnetic axis that is side-looking. The end-looking optical axis made achievement of low backgrounds easier, because a longer working distance for field-of-view limiting is more conveniently available than with a side-looking optical axis. The sample is positioned at 45° to both axes, as shown in Figure 1. This is the only simple means of doing both the electrical and optical measurements. The losses involved were not too great, since 70% ($\cos 45^\circ$) of the maximum achievable for both the optical response and Hall voltage was obtained.

The aperture plate on the sample chamber is rotatable so that the apertures, and thus chamber backgrounds, can be changed. Rotation is accomplished by studs on the aperture plate that are captured by holes in a plate attached to the Cryotip end piece. This end piece is attached to the body of the Cryotip by O-rings and is manually rotatable. When it

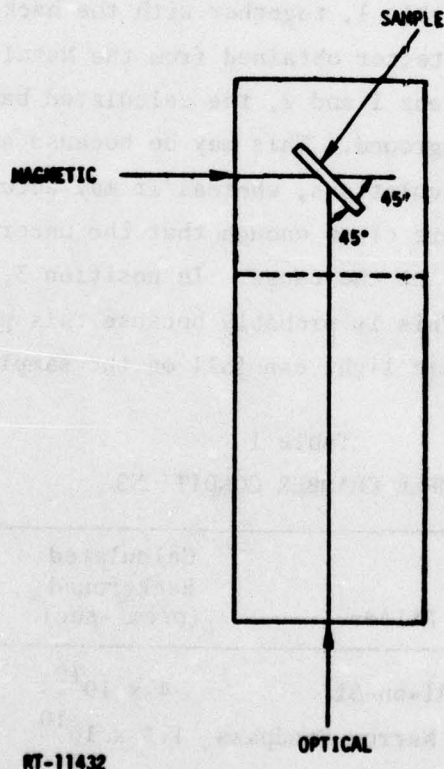


Figure 1. Orientation of sample with respect to the optical and magnetic axes

rotates, the aperture plate does also. Once the desired rotation is accomplished, the end piece is backed off slightly to disconnect it mechanically from the cold aperture plate and prevent a thermal leak. There are four positions in the aperture plate. A fixed aperture below the rotatable aperture plate sets which position is being used and thus the condition in the chamber. The first position is an 0.02-inch-diameter aperture covered by a filter that is aluminum-evaporated on silicon. The transmission characteristics of this filter are shown in Figure 2. The second position is an 0.05-inch-diameter aperture covered by a 4.1- μm narrow-bandpass filter, the transmission characteristics of which are shown in Figure 3. The third position is an uncovered 0.1-inch-diameter aperture, and the fourth position is closed off. The apertures are three inches from the sample location. Using the known field-of-view and transmission characteristics of the filters, the background in the chamber under the various conditions can be calculated. These calculated values are shown in Table 1, together with the background measured using a calibrated silicon detector obtained from the Naval Electronics Laboratory Center. In positions 1 and 2, the calculated background is higher than the measured background. This may be because an emissivity of 1.0 was assumed in the calculations, whereas it may actually have been less. However, the numbers are close enough that the uncertainties in the measurements may actually be the cause. In position 3, the measured background is much higher. This is probably because this position is the only one in which intrinsic light can fall on the sample. The response

Table 1
SAMPLE CHAMBER CONDITIONS

Position	Aperture Diameter (inches)	Filter	Calculated Background (p/cm ² -sec)	Measured Background (p/cm ² -sec)
1	0.02	Al-on-Si	4×10^{10}	2×10^{10}
2	0.05	4.1- μm Narrow Bandpass	1.3×10^{10}	1×10^{10}
3	0.10	None	6×10^{14}	5×10^{15}
4	Blank	--	--	2×10^9

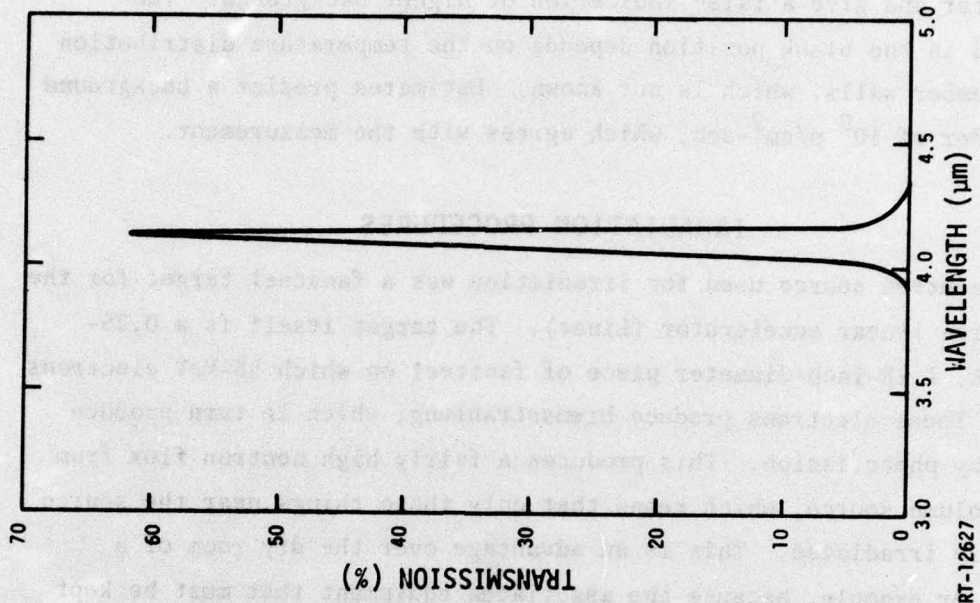


Figure 3. Transmission of 4.1- μ m narrow-bandpass filter

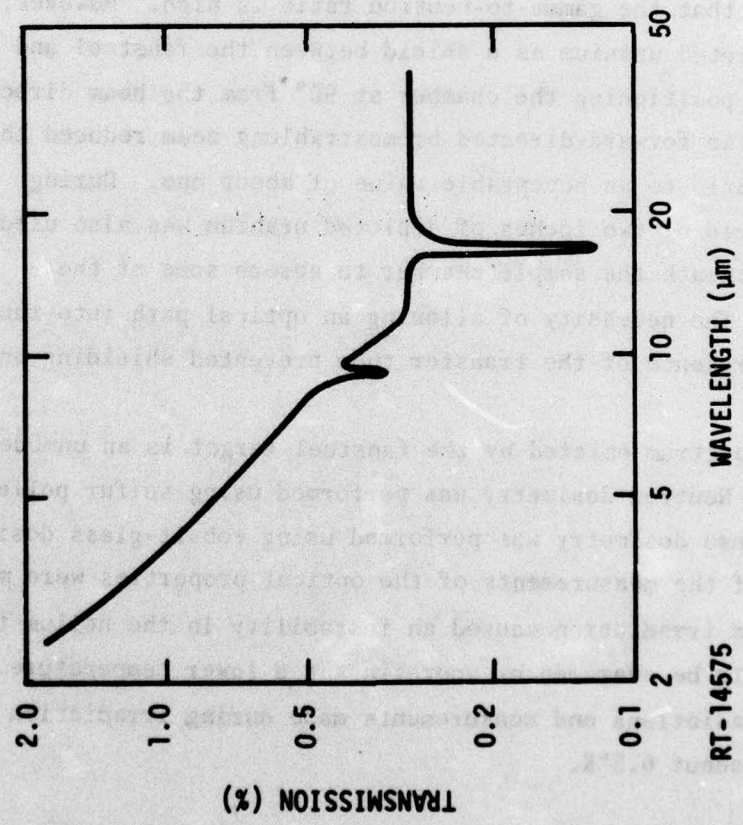


Figure 2. Transmission of the Al-on-Si filter

of the calibrated background detector to the intrinsic light would be much greater and give a false indication of higher background. The background in the blank position depends on the temperature distribution in the chamber walls, which is not known. Estimates predict a background of the order of 10^9 p/cm²-sec, which agrees with the measurement.

IRRADIATION PROCEDURES

The neutron source used for irradiation was a fansteel target for the IRT electron linear accelerator (Linac). The target itself is a 0.25-inch-thick, 1.25-inch-diameter piece of fansteel on which 55-MeV electrons impinge. These electrons produce bremsstrahlung, which in turn produce neutrons by photofission. This produces a fairly high neutron flux from a small volume source, which means that only those things near the source are heavily irradiated. This is an advantage over the dry room of a reactor, for example, because the associated equipment that must be kept near the cryostat does not become as activated. One disadvantage of the fansteel source is that the gamma-to-neutron ratio is high. However, use of 4 inches of depleted uranium as a shield between the fansteel and the sample chamber and positioning the chamber at 90° from the beam direction to remove it from the forward-directed bremsstrahlung beam reduced the gamma-to-neutron ratio to an acceptable value of about one. During irradiation, a shield of two inches of depleted uranium was also used on two sides and beneath the sample chamber to absorb some of the scattered gammas. The necessity of allowing an optical path into the cryostat and the presence of the transfer tube prevented shielding on all four sides.

The neutron spectrum emitted by the fansteel target is an unmoderated fission spectrum. Neutron dosimetry was performed using sulfur pellet dosimeters, and gamma dosimetry was performed using cobalt-glass dosimeters.

Though most of the measurements of the optical properties were made at 11°K ($\pm 1^\circ$ K), the irradiation caused an instability in the helium transfer which could only be overcome by operating at a lower temperature. Therefore, the irradiations and measurements made during irradiation were performed at about 6.5°K.

Measurements made during irradiation were made remotely because of the high radiation level in the target room. Therefore, only one background condition in the sample chamber could be used. This was chosen to be the 4.1- μm filter because the low background response degradation was most important. Measurements as a function of irradiation were made both with the irradiation beam on and with it off, so both high- and low-injection measurements were obtained. Only the optical response could be measured because the sample resistance at the low background and temperature was much higher than the leakage resistance in the cryostat feedthroughs, and no meaningful electrical properties data could be obtained.

MEASUREMENT PROCEDURES

Electrical and optical properties of the samples were measured in fairly typical fashion. Samples were cut in bars and contacts fastened in a bridge configuration, as shown in Figure 4. For electrical properties measurements, the current is passed between contacts A and B, the resistivity voltage is measured between adjacent contacts on the

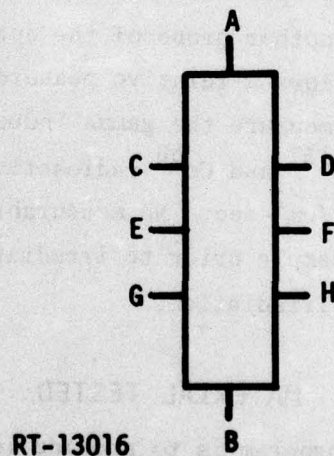


Figure 4. Sample geometry. (The lettered points are used in Table 2 where sample dimensions are listed.)

same side (e.g., C and E), and the Hall voltage is measured between opposite contacts (e.g., E and F). The electrical properties were measured as a function of temperature from room temperature (or the anneal temperature during annealing experiments) down to the lowest temperature at which good measurements could be made (about 20°K).

Optical response measurements can be made in a number of configurations: in the normal resistivity configuration (between contacts A and B directly); across the sample between pairs of Hall voltage contacts (e.g., C,E and D,F); or along the sample between pairs of resistivity voltage contacts (e.g., C,D and E,F). In this way, the dependence of the response on sample length could be examined.

The optical source used for response measurements was a blackbody operated at 1000°K. Response measurements were made using the source with both the 4.1- μ m filter and the Al-on-Si filter. For the spectral dependence measurements, a Spex grating monochromator with a globar light source was used. These measurements were made using both the open hole and the Al-on-Si filter to examine differences between measurements at high and low background.

One other measurement was made. This was to measure the electrical properties at 11°K, using the open hole and the 1000°K blackbody as an injection source. This is another probe of the optical generation and recombination process and allows a relative measure of the lifetime.

An attempt was made to measure the gamma-induced noise and pulses in the samples using both Cs¹³⁷ and Co⁶⁰ radioactive sources. The fluxes were as high as 10^6 γ/cm^2 -sec. No measurable gamma-induced effect was observed in any sample prior to irradiation, and this measurement was not made following irradiation.

MATERIAL TESTED

Since the aim of this program is to provide information concerning the vulnerability of LWIR detectors, material which is similar to that from which quality detectors are made should be tested. State-of-the-art detectors have a thickness of about 0.1 mm, and this requires an

arsenic concentration of about $5 \times 10^{16} \text{ cm}^{-3}$ for sufficient light absorption. This is not necessarily a magic number, however, because detector thickness can vary, and thus the arsenic concentration requirement changes. What is more important is that other undesirable electrically active impurities be low in concentration. A high acceptor concentration would compensate a large number of arsenic sites and decrease the lifetime and thus the photoconductive response. A high concentration of donors with levels shallower than the As level would mean that significant thermal carrier generation would exist at temperatures below where the As carriers are frozen out. Additionally, material with high mobility is necessary because the photoconductive response is actually set by the mobility-lifetime product.

Si:As material was obtained from Aerojet ElectroSystems Company and Rockwell International, both of whom fabricate and supply high-quality LWIR detectors. The Aerojet material was supplied in several wafers that were labeled either X105 - 6.5 cm or X105 - 55 mm. The Aerojet material is pulled crystal or high oxygen concentration. Though the wafers were not actually tested by Aerojet, they were from crystals from which quality detectors were made. The material used on this program was from the wafer labeled X105 - 6.5 cm and had a nominal room temperature carrier concentration (which equates to the As concentration) of $4 \times 10^{16} \text{ cm}^{-3}$. The Rockwell material was also supplied in two wafers, both labeled HPT307025A. The wafers were then labeled slice B1 or B2 with B2 being used. The Rockwell material is float-zone refined or low oxygen concentration. The nominal room temperature resistivity was $0.269 \Omega \text{ cm}$, which means an As concentration of $2.2 \times 10^{16} \text{ cm}^{-3}$. Again, the wafers had not been tested by Rockwell, but quality detectors had been fabricated from material from this crystal.

In addition to the above material, IRT had a boule of Si:As which was previously obtained from High Performance Technology (HPT). HPT was a supplier of Si:As to LWIR detector manufacturers before it went out of business. This boule was float-zone refined or low oxygen concentration. It has a nominal arsenic concentration of 10^{16} cm^{-3} and

low concentrations of other unwanted impurities. IRT has previously fabricated 1 mm^3 detectors of high quality from the material.

Bar samples were cut from the wafers with a diamond saw. The samples were then polished, etched with CP-4, and As-doped gold contacts alloyed to the bar in a bridge configuration.

In general, only one sample of each type material was tested. However, a Rockwell sample was the first tested, and a number of experimental difficulties left the results open to questions, so a second sample of this material was subsequently tested. The primary experimental difficulty during the first test was a loose optical mirror that caused the response measurements to vary significantly. Also, temperature control was not as tight as necessary during the electrical properties measurements, and the resulting data scatter was unacceptably large. Further, it was not realized until the performance of this experiment that the neutron irradiation would produce instabilities in the helium transfer system, necessitating operation at lower temperature. Therefore, when such instabilities occurred during the irradiation, it was necessary to cool the chamber more and continue the irradiation at a lower temperature where no prior measurements had been made. This meant normalizations were required and added another question to the results. As a result of all these factors, the data from this initial sample are not considered in this report.

ANALYTICAL CONSIDERATIONS

To examine the mechanisms involved in the neutron damage of Si:As, it is necessary to determine the basic physics parameters of the material. However, these are not measured directly, and one must determine the relationship between the measured quantities and the material parameters.

DEPENDENCE OF ELECTRICAL PROPERTIES ON MATERIAL PARAMETERS

When measuring the electrical properties of a material, one measures the resistivity, ρ , (or the conductivity, σ) and the Hall coefficient, R_H (from which can be obtained the carrier concentration, $n = 1/R_H e$). The dependence of these quantities on the material parameters has been dealt with extensively (Ref. 97) and the results are well understood. In Si:As, we are dealing with an n-type semiconductor with N_d donors (activation energy E_d) and N_a compensating acceptors. From room temperature down to nitrogen temperature, all the uncompensated donors are excited, and the carrier concentration is

$$n = N_d - N_a \quad (1)$$

For $N_d \gg N_a$, this is $n = N_d$. (2)

As the temperature is lowered, carriers freeze out on the donor sites. So long as $n \gg N_a$, the acceptors have little effect, and the carrier concentration is given by

$$n = (\beta N_c N_d)^{1/2} e^{-E_d/2kT} \quad (3)$$

where β^{-1} is the degeneracy of a donor level and N_c is the density of states in the conduction band. At lower temperatures yet, N_a becomes larger than n , and the carrier concentration is given by

97. See for example: J. S. Blakemore, "Semiconductor Statistics," Pergamon Press, (1962).

$$n = \beta N_C \frac{(N_d - N_a)}{N_a} e^{-E_d/kT} \quad (4)$$

The slope of the carrier concentration versus inverse temperature (allowing for the $T^{3/2}$ dependence of N_C) in either region gives E_d . Knowing N_d from the higher-temperature measurements, both β and N_a can be determined.

Eventually, the thermal generation of carriers will drop enough so that the optical generation will set the carrier concentration. Below this temperature, the carrier concentration again becomes constant as long as the lifetime remains constant.

The mobility (μ) of the material can also be determined from

$$\alpha = n e \mu \quad (5)$$

The mobility depends inversely on the scattering of the carriers, which depends directly on the number of scattering centers. The scattering also depends on the charge on the centers, making calculations difficult. The mobility can be written as

$$\frac{1}{\mu} = f(q^{-2}) N_s \quad (6)$$

where $f(q^{-2})$ is a proportionality constant that depends on the mean square of the charge on the centers. It also could depend on temperature or other variables, but this is not important to the subsequent discussion. Note that $f(0) \neq 0$ because neutral centers scatter also and that $f(q)$ may differ for different types of centers even if they have the same charge.

DEPENDENCE OF PHOTOCONDUCTIVITY ON MATERIAL PARAMETERS

The general expression for the responsivity (at frequencies above where dielectric relaxation occurs) of a sample is

$$I_\lambda = \eta_\lambda G \frac{q\lambda}{hc} \quad (7)$$

where

- η_λ is the quantum efficiency,
- G is the photoconductive gain, and
- λ is the measurement wavelength.

The dependence of η_λ now needs to be examined.

$$\eta_\lambda \approx 1 - \exp(-\sigma N_d d) \quad , \quad (8)$$

where

σ is the cross section,

N_d is the number of centers capable of absorbing light, and

d is the detector thickness.

Thus,

$$I_\lambda \approx G \frac{q\lambda}{hc} [1 - \exp(-\sigma N_d d)] \quad . \quad (9)$$

For $\sigma N_d d \gg 1$,

$$I_\lambda \approx G \frac{q\lambda}{hc} \quad , \quad (10)$$

since the term in brackets is essentially unity. For $\sigma N_d d \ll 1$, the term in brackets becomes $\sigma N_d d$, and

$$I_\lambda \approx G \frac{q\lambda}{hc} \sigma N_d d \quad , \quad (11)$$

In the case of most silicon LWIR detectors, $\sigma N_d d$ will be between the extremes. However, since the material used here is the same as that from which detectors are made and the samples used are somewhat thicker, $\sigma N_d d$ will be greater than 1, and Equation 10 should be used; however, use of Equation 9 will cover all cases.

The dependence of the photoconductive gain below saturation (at low bias) has the form

$$G = \left(\frac{\mu\tau_n}{E} \right) \frac{V^2}{\ell^3} \quad (12)$$

or

$$G = \frac{\mu\tau_n V}{\ell^2} \quad , \quad (13)$$

where τ_n is the majority-carrier lifetime and μ is the mobility, depending on whether $\mu\tau$ depends on E or not. A V^2 dependence of the response indicates that $\mu\tau$ does depend on E and that Equation 13 holds. For radiation effects, this is of secondary importance, and the fact that G (and thus, the response) depends on τ_n is most important. Thus, the responsivity equation has the form

$$I_\lambda = \frac{q\lambda}{hc} \frac{V}{\ell^2} \eta_\lambda \mu \tau_n \quad (14)$$

In the saturation region (high bias) and since we are operating at frequencies where dielectric relaxation cannot occur, G is limited to $1/2$ (or perhaps some other constant) and the responsivity can be written as

$$I_\lambda = \frac{q\lambda}{2hc} \eta_\lambda \quad (15)$$

The basic material parameters in these equations which can be changed by irradiation are the majority-carrier lifetime (τ_n), the mobility (μ), and the number of centers capable of absorbing light (N_d). Writing the responsivity in terms of these parameters gives

$$I_\lambda \propto [1 - \exp(-\sigma N_d d)] \mu \tau_n \quad \text{at low bias} \quad (16)$$

or

$$I_\lambda \propto [1 - \exp(-\sigma N_d d)] \quad \text{at high bias} \quad (17)$$

IRRADIATION-INDUCED CHANGES IN MATERIAL PARAMETERS

It is now necessary to determine how irradiation changes the material parameters and then how these changes affect measured properties. The basic effect of irradiation is the production of defect complexes, which can do a number of things to the material. For example, if the complexes include the optically active impurity atoms, the atoms will no longer be capable of providing optical response. If the complexes remove carriers from the optically active impurity atoms, not only will those atoms not be able to provide optical response, but also they will be an additional recombination location for majority carriers. The defect complexes

themselves can act as minority- or majority-carrier recombination centers or be scattering sites to affect the carrier mobility. The defect complexes are usually introduced at a rate which is linear with fluence (Φ).

The introduction of defects can be written as

$$N = \frac{dN}{d\Phi} \Phi , \quad (18)$$

where N is the number of defects and $dN/d\Phi$ is the introduction rate. If only majority-carrier removal sites are introduced, this defect introduction rate would be akin to the room-temperature carrier removal rate ($dn/d\Phi$).

The lifetime of a material is the property most readily affected by irradiation. For the minority-carrier lifetime, this is because radiation defects seem to have larger recombination cross sections than defects already present, such as impurity atoms. For the majority-carrier lifetime, this is because quality detector material operated at low temperature and background and closely compensated has few unoccupied sites at which recombination can occur. The lifetime of a material depends inversely on the number of recombination centers available:

$$\tau = \frac{1}{\sigma v N_R} , \quad (19)$$

where

σ is the capture cross section,

v is the carrier velocity, and

N_R is the concentration of available recombination centers.

For multiple recombination centers,

$$\frac{1}{\tau} = \sum_i \frac{1}{\tau_i} = \sum_i \sigma_i v N_{R_i} . \quad (20)$$

As irradiation adds new recombination centers, the lifetime changes can be written as

$$\frac{1}{\tau} = \frac{1}{\tau_0} + \sigma_d v \frac{dN}{d\Phi} \Phi = \frac{1}{\tau_0} + K_\tau \Phi , \quad (21)$$

where τ_0 is the initial lifetime and K_τ is the lifetime degradation constant. Writing this in normalized form gives

$$\frac{\tau}{\tau_0} = \frac{1}{1 + K_\tau \tau_0 \Phi} \quad (22)$$

For the majority-carrier lifetime where the irradiation simply introduces more of the same recombination centers (empty optical donor sites), and thus $\sigma_0 = \sigma_d$, the normalized form can be written in terms of the defect introduction rate as

$$\frac{\tau_n}{\tau_{n0}} = \frac{1}{1 + \frac{1}{N_+} \frac{dN}{d\Phi} \Phi} \quad (23)$$

where N_+ is the initial number of unoccupied (positive) optically active levels.

The effect of irradiation on the number of absorbing centers is simply a removal of them, which can be written as

$$N = N_0 - \frac{dN}{d\Phi} \Phi \quad (24)$$

where N_0 is the initial number of occupied (neutral) optically active levels and is equal to N_d in these materials. This is less sensitive than the lifetime, since the number of defects introduced must become significant compared with the number of absorbing centers initially present (N_0) before any effect is observed. Since the number of absorbing centers is orders of magnitude larger than the number of recombination sites (N_+) in high-quality detector material, the lifetime is much more sensitive.

Upon irradiation, the mobility will change as

$$\frac{1}{\mu} = \frac{1}{\mu_0} + f_d(q^{-2}) \frac{dN}{d\Phi} \Phi = \frac{1}{\mu_0} + K_\mu \Phi \quad (25)$$

where K_μ is the mobility degradation constant. This is very similar to the lifetime equation (Equation 21) and can be written in normalized form as

$$\frac{\mu}{\mu_0} = \frac{1}{1 + \mu_0 K_\mu \Phi} \quad (26)$$

The mobility is less sensitive to irradiation than the majority-carrier lifetime, since there is a significant number of scattering centers present in the detectors compared with the number of recombination sites available. Since the mobility always enters the analysis as a product with the majority-carrier lifetime, it does not govern detector changes to a large extent.

IRRADIATION-INDUCED CHANGES IN ELECTRICAL PROPERTIES AND PHOTOCONDUCTIVITY

The introduction of defects in the material is effectively the addition of compensating acceptors. This would first affect the electrical properties by decreasing the low-temperature-carrier concentration in the region where N_a controls it. The decrease in n at any temperature will be proportional to the increase in N_a . If the defect concentration becomes high enough, the value of $N_d - N_a$ would drop, and the high-temperature-carrier concentration would also decrease.

The additional defects will also produce additional scattering and lower the mobility. The change in scattering can be examined only qualitatively because of the differences between different types of scattering centers.

The low bias responsivity can be written in normalized form as

$$\frac{I_\lambda}{I_{\lambda_0}} = \frac{\eta_\lambda}{\eta_{\lambda_0}} \frac{\mu}{\mu_0} \frac{\tau_n}{\tau_{n_0}} \quad (27)$$

Since the lifetime is the most sensitive parameter, this can be written as

$$\frac{I_\lambda}{I_{\lambda_0}} = \frac{\tau_n}{\tau_{n_0}} \quad (28)$$

Substituting Equation 22 gives

$$\frac{I_\lambda}{I_{\lambda_0}} = \frac{1}{1 + K_\tau \tau_0 \Phi} \quad (29)$$

or Equation 23 gives

$$\frac{I_{\lambda}}{I_{\lambda_0}} = \frac{1}{1 + \frac{1}{N} \frac{dN}{d\Phi} \Phi} \quad (30)$$

At high bias, the responsivity in normalized form is

$$\frac{I_{\lambda}}{I_{\lambda_0}} = \frac{\eta_{\lambda}}{\eta_{\lambda_0}} \quad (31)$$

For $\sigma N_d d \gg 1$, this is independent of any material parameter and would not change with fluence. Eventually, enough removal would occur that $\sigma N_d d \ll 1$ would be valid and

$$\frac{I_{\lambda}}{I_{\lambda_0}} = \frac{N}{N_0} \quad (32)$$

Substituting Equation 24 gives

$$\frac{I_{\lambda}}{I_{\lambda_0}} = 1 - \frac{1}{N_0} \frac{dN}{d\Phi} \Phi \quad (33)$$

One apparent change in electrical properties, which is actually a photoconductivity change, is a carrier concentration decrease at low temperatures where n is set by optical background generation. Thus, the carrier concentration is actually a measure of the steady-state photoconductivity, and majority carrier lifetime degradation would decrease the carrier concentration.

EXPERIMENTAL RESULTS

PREIRRADIATION CHARACTERIZATION

The material properties of samples cut from the various wafers were characterized prior to irradiation. The sample dimensions are shown in Table 2. The carrier concentration results are shown in Figure 5.

Table 2
DIMENSIONS OF THE Si:As SAMPLES^a

	Rockwell	Aerojet	HPT
Length (A-B)	0.417 cm	0.946 cm	0.903 cm
Resistivity Dimension (C-E)	0.108 cm	0.323 cm	0.323 cm
Width (E-F)	0.0344 cm	0.138 cm	0.0387 cm
Thickness	0.0602 cm	0.120 cm	0.0731 cm

^aSee Figure 4 for sample location of the lettered points.

The material parameters calculated from these data are given in Table 3.

Table 3
MATERIALS PARAMETERS OF THE Si:As SAMPLES AS DETERMINED FROM THE CARRIER CONCENTRATION

Material Source	As Concentration N_d (cm^{-3})	Activation Energy E_d (eV)	Degeneracy Factor, β	Acceptor Concentration N_a (cm^{-3})
Rockwell	2.2×10^{16}	0.053	0.5	5.3×10^{13}
Aerojet	3.1×10^{16}	0.054	0.5	6.2×10^{13}
HPT	1.9×10^{16}	0.054	0.5	5.2×10^{13}

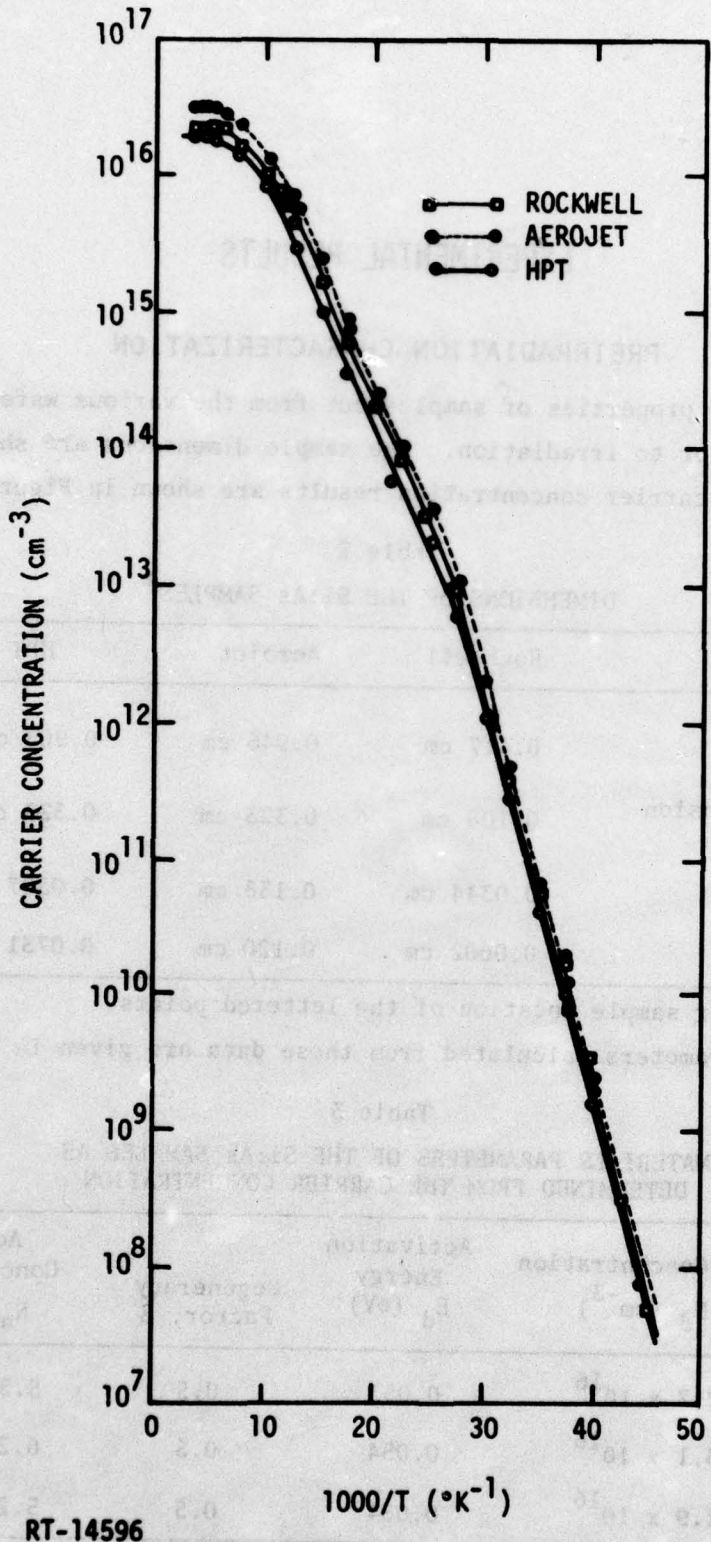


Figure 5. Carrier concentration of the Si:As samples

The arsenic concentrations are quite accurate, being very easy to measure and not depending on another measured parameter. The energy levels varied by 0.001 eV between the higher temperature $E_d/2kT$ region and the lower temperature E_d/kT region for the various samples. Also the scatter in the data would allow the drawing of a line with a slope that differed by up to 0.001 eV from the one listed in Table 3. The value for the Rockwell material seemed to be slightly lower (shallower slope) than for the other two. Although, since they were all the As level, they should have been the same. If the activation energy of the Rockwell sample were forced to be 0.054 eV, the calculated acceptor concentration would be lowered to $3.3 \times 10^{13} \text{ cm}^{-3}$ or significantly lower than the others. The calculated degeneracy factor ranged from 0.4 to 0.6. Since β^{-1} must be either 1, 2, or 4 (in principle, it could be any even number), the value of β is almost certainly 0.5. The experimental data can be fit reasonably by other combinations of parameters (in particular of E_d and N_a) than shown in Table 3. Although exhaustive fitting attempts were not made, it seemed that changes in E_d of greater than ± 0.001 would not result in reasonable fits. This puts a limit to the N_a values as being within a factor of two of the values listed. A specific point is that an attempt to force the acceptor concentration to be 10^{13} cm^{-3} (the value where the break in the curves in Figure 5 occurs) results in an activation energy of about 0.058 eV, which appears much too steep to fit the data. In any event, the relative values for a given sample are quite accurate, and this is probably more important than absolute accuracy.

The material parameters listed in Table 3 are slightly different from those given in earlier status reports. These differences are a measure of the accuracy of the results, because the data can be fit reasonably by either the previous or the present parameters. However, it is felt that the present parameters are more accurate because they were determined by comparing the data from all three samples, primarily so as to choose a reasonably consistent activation energy. The prior parameters were determined from the data on the sample in question only.

The impurity concentrations were not as different as could be desired for a good study of damage dependence on this variable. Neither the Rockwell nor the Aerojet material had an As concentration as high as it might have been, though both were acceptable. The HPT sample had

an As concentration about twice what was expected. Other samples with As concentrations of about $1 \times 10^{16} \text{ cm}^{-3}$ had been cut from the boule. However, this sample was contacted and mounted late in the program, and there was not enough time or effort available to cut another sample from a different location to determine if a lower concentration would be obtained.

The mobility of the various samples is shown in Figure 6. At temperatures above about 80°K , the mobilities are very similar. The temperature dependences are all approximately $T^{-3/2}$, though the HPT material seems to be slightly steeper. In this region, the mobility is set by lattice scattering. As the temperature is decreased, the slope of the line becomes greater for some reason, and then the mobility levels out below about 40°K . It is in this region that ionized or neutral impurity scattering predominates. The ordering of the Rockwell and Aerojet materials in this region is reasonable, since the Rockwell material has a lower donor, acceptor, and oxygen concentration; therefore, both the ionized and neutral impurity scattering would be less and the mobility higher. However, HPT sample had a significantly higher mobility than the others, even though its acceptor concentration (and, thus, its ionized impurity concentration) was about the same as the others and its oxygen concentration (and, thus, its neutral impurity concentration) was lower than that of the Aerojet material. Since the mobility ordering is the inverse of the As concentration ordering, this perhaps indicates that the low-temperature scattering is dominated by the neutral arsenics. However, it is more likely that the reason is differences in dislocation density or some other unmeasured quantity.

The spectral dependence of the response of the samples is shown in Figure 7. The response is relatively typical of Si:As detectors, increasing with wavelength at a rate closer to λ^2 than λ^1 , as an ideal photoconductor would do when the normalization is to the incident power. The reason is because the samples are not thick, and at shorter wavelengths where the absorption coefficient is lower, a smaller fraction of the light is absorbed; this serves to decrease the response.

The HPT sample had a steeper wavelength dependence than the other two for a reason that is not understood. This is expected for less heavily doped material, which the HPT sample was, but the doping difference involved was not enough to cause the effect seen. Further, the doping

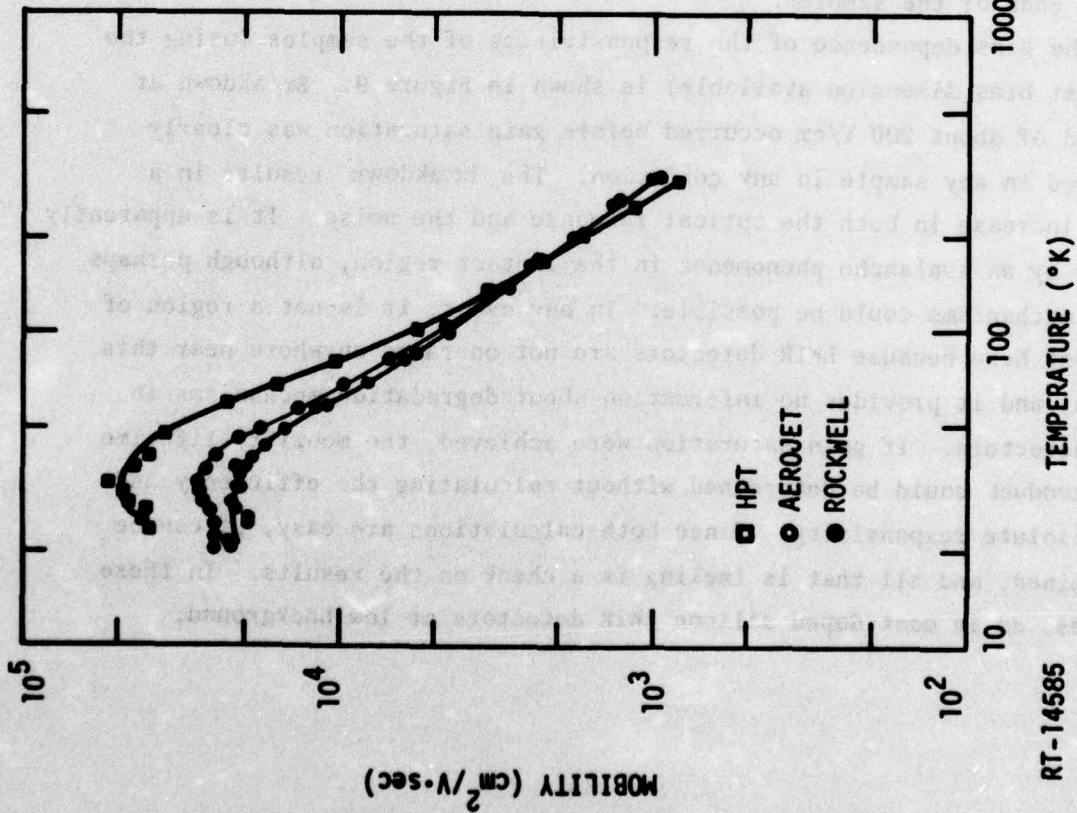


Figure 6. Mobility of the Si:As samples

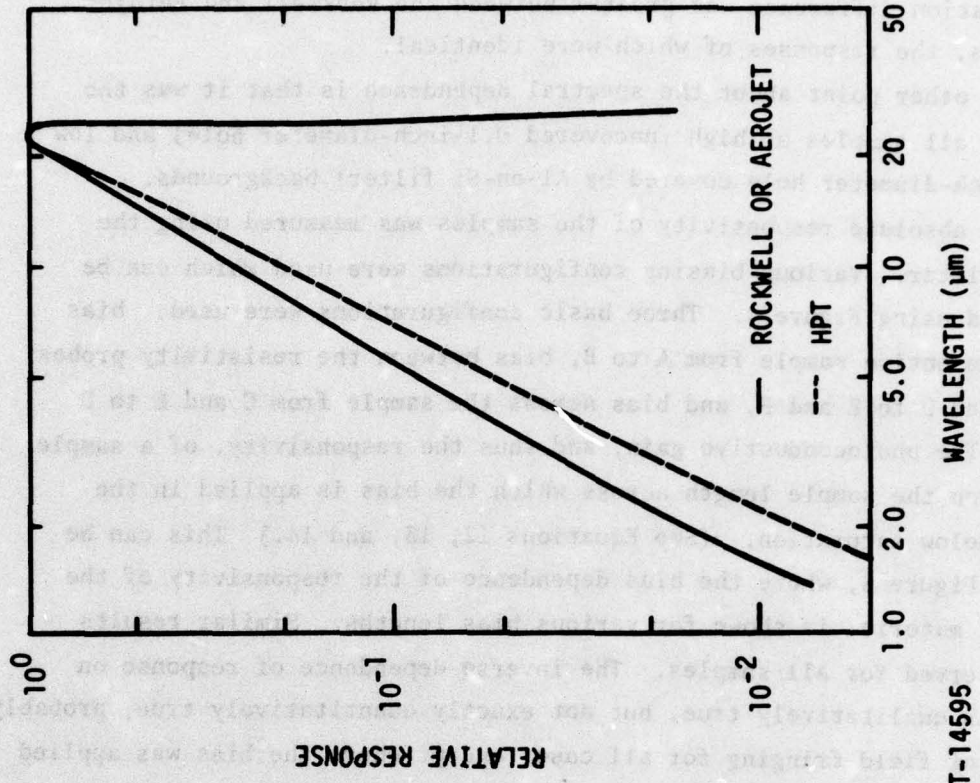


Figure 7. Wavelength dependence of the response of Si:As samples. (Normalized to incident power)

concentration difference was greater between the Rockwell and Aerojet materials, the responses of which were identical.

One other point about the spectral dependence is that it was the same for all samples at high (uncovered 0.1-inch-diameter hole) and low (0.02-inch-diameter hole covered by Al-on-Si filter) backgrounds.

The absolute responsivity of the samples was measured using the 4.1- μm filter. Various biasing configurations were used which can be explained using Figure 4. Three basic configurations were used: bias along the entire sample from A to B, bias between the resistivity probes from C and D to E and F, and bias across the sample from C and E to D and F. The photoconductive gain, and thus the responsivity, of a sample depends on the sample length across which the bias is applied in the region below saturation. (See Equations 12, 13, and 14.) This can be seen in Figure 8, where the bias dependence of the responsivity of the Rockwell material is shown for various bias lengths. Similar results were observed for all samples. The inverse dependence of response on length is qualitatively true, but not exactly quantitatively true, probably because of field fringing for all cases except where the bias was applied to the ends of the samples.

The bias dependence of the responsivities of the samples (using the shortest bias dimension available) is shown in Figure 9. Breakdown at a field of about 200 V/cm occurred before gain saturation was clearly achieved in any sample in any condition. The breakdown results in a large increase in both the optical response and the noise. It is apparently caused by an avalanche phenomenon in the contact region, although perhaps other mechanisms could be possible. In any event, it is not a region of interest here because LWIR detectors are not operated anywhere near this region, and it provides no information about degradation mechanisms in such detectors. If gain saturation were achieved, the mobility-lifetime ($\mu\tau$) product could be determined without calculating the efficiency and the absolute responsivity. Since both calculations are easy, $\mu\tau$ can be determined, and all that is lacking is a check on the results. In these samples, as in most doped silicon LWIR detectors at low background,

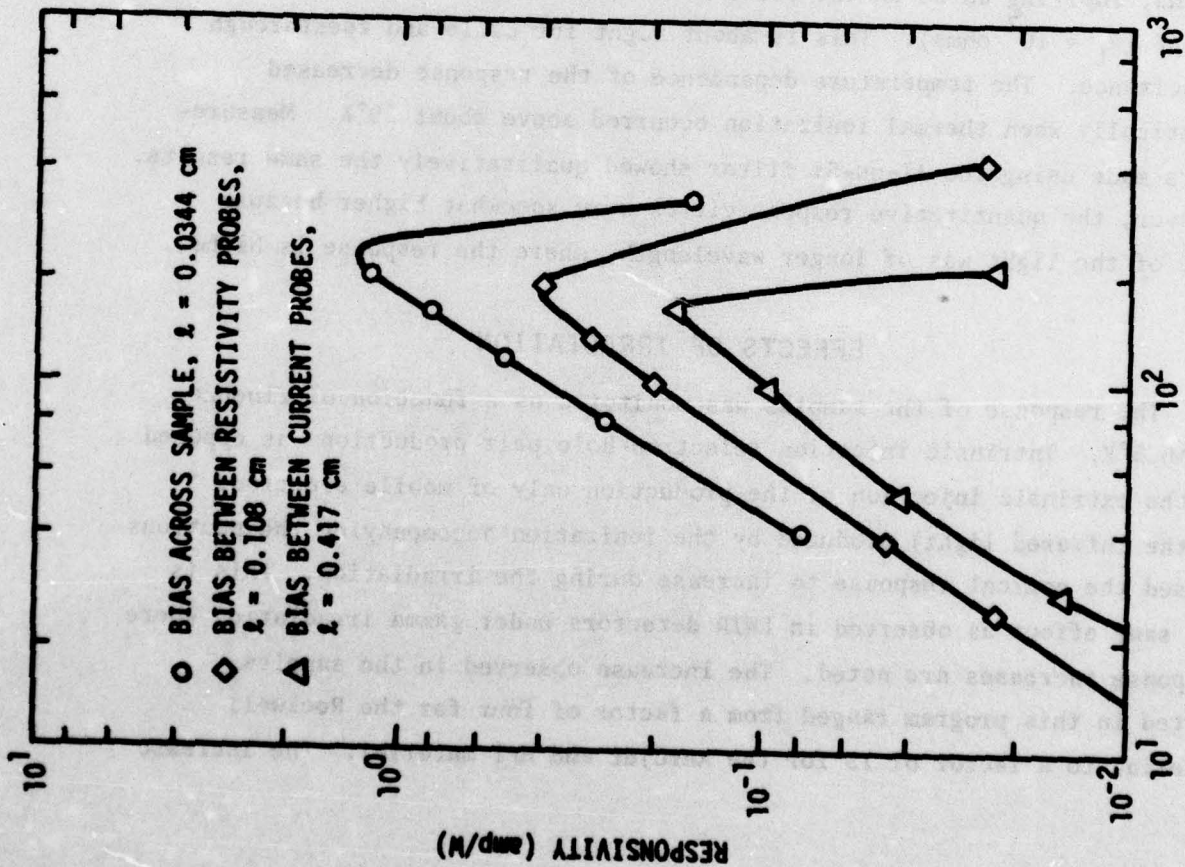


Figure 8. Length dependence of the responsivity of the Autonetics sample prior to irradiation, $\lambda = 4.1 \mu\text{m}$

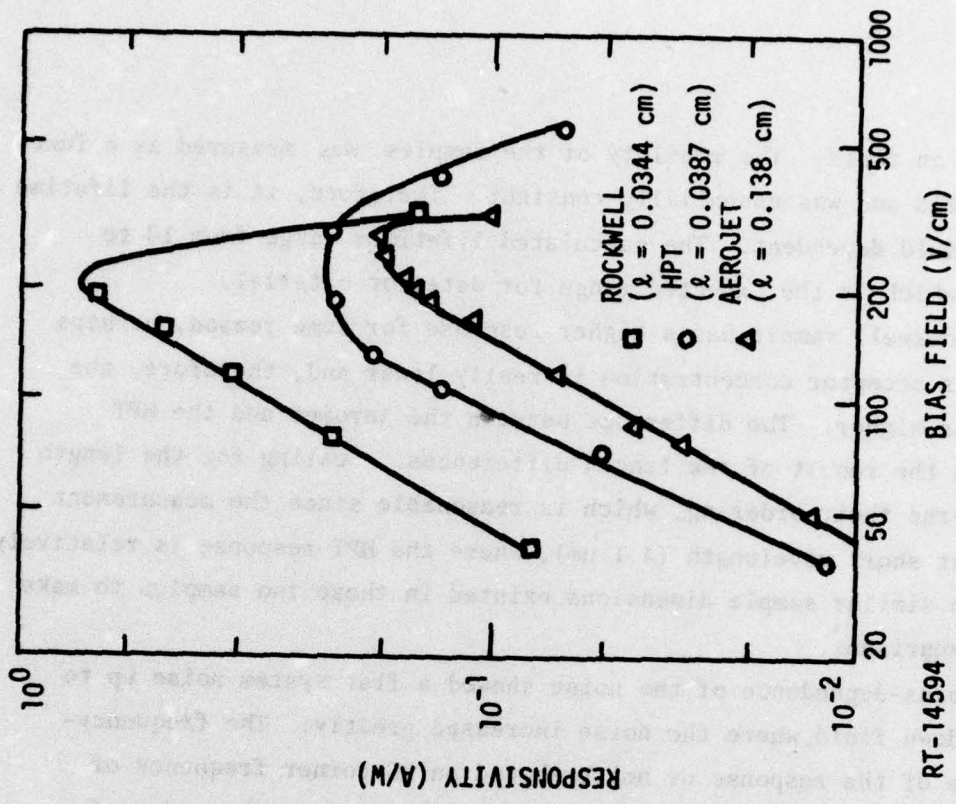


Figure 9. Responsivity of the Si:As samples, $\lambda = 4.1 \mu\text{m}$

$\mu\tau$ depends on field. The mobility of the samples was measured as a function of field and was essentially constant. Therefore, it is the lifetime which is field dependent. The calculated lifetimes range from 10 to 100 nsec, which is the expected range for detector material.

The Rockwell sample has a higher response for some reason, perhaps because its acceptor concentration is really lower and, therefore, the lifetime is higher. The difference between the Aerojet and the HPT sample was the result of the length differences. Scaling for the length would reverse their ordering, which is reasonable since the measurement was made at short wavelength ($4.1 \mu\text{m}$), where the HPT response is relatively lower. No similar sample dimensions existed in these two samples to make direct comparisons.

The bias-dependence of the noise showed a flat system noise up to the breakdown field, where the noise increased greatly. The frequency-dependence of the response or noise showed an RC corner frequency of 100 Hz, implying an RC on the order of 1.5 msec or C on the order of 150 pF ($R_L = 10^7$ ohms). This is about right for cable and feedthrough capacitance. The temperature dependence of the response decreased drastically when thermal ionization occurred above about 20°K . Measurements made using the Al-on-Si filter showed qualitatively the same results. However, the quantitative responsivities were somewhat higher because some of the light was of longer wavelength, where the response is higher.

EFFECTS OF IRRADIATION

The response of the samples was monitored as a function of fluence at $\sim 6.5^\circ\text{K}$. Intrinsic injection (electron-hole pair production as opposed to the extrinsic injection or the production only of mobile electrons by the infrared light) produced by the ionization accompanying the neutrons caused the optical response to increase during the irradiation. This is the same effect as observed in LWIR detectors under gamma irradiation where response increases are noted. The increase observed in the samples tested in this program ranged from a factor of four for the Rockwell material to a factor of 15 for the Aerojet and HPT material. The increase

apparently is a result of the excess carriers produced by the intrinsic injection, perhaps by field redistribution across the sample, although this is not really known and is the subject of much study at present. In any event, since the effect depends in some way on the injection of carriers in an intrinsic process, it may depend on the intrinsic lifetime as well as the majority-carrier lifetime, which governs the optical response. Lacking a model of the dependence means that no quantitative information about material parameters can be obtained from the measured degradation rate under intrinsic injection. However, it was measured, as well as the no-intrinsic-injection degradation, to provide information for use in the developing theories.

To measure the degradation with no intrinsic injection, the Linac was shut off and the bias dependence of the response measured after the intrinsic-injection-induced increase had decayed away. An example of these results is shown in Figure 10 for the Aerojet sample. All samples showed similar results. The measurements were made at low field so that any confusion caused by effects near breakdown would not be encountered. From these results, the degradation rate of the response can be found. The normalized results are shown in Figures 11 and 12 for the cases of no intrinsic injection and intrinsic injection, respectively. The points are the measured data and the lines are fits to the analytical Equations 29 and 30 with mobility changes allowed for, as will be explained subsequently.

The electrical properties were not measured as a function of fluence, but only before and after irradiation. In fact, to determine some of the material parameters from the electrical properties, the samples had to be heated to the first annealing point ($\sim 40^\circ\text{K}$). As will be shown in the next section, little if any annealing of the optical properties occurred during this process, so the parameters are valid numbers for the post-irradiation values. As expected, the carrier concentration of the samples decreased, while the activation energy remained unchanged. This means that additional acceptors were introduced by the irradiation. The mobility also showed some slight decrease, indicating the introduction of additional scattering centers. An introduction rate of acceptors and a mobility degradation

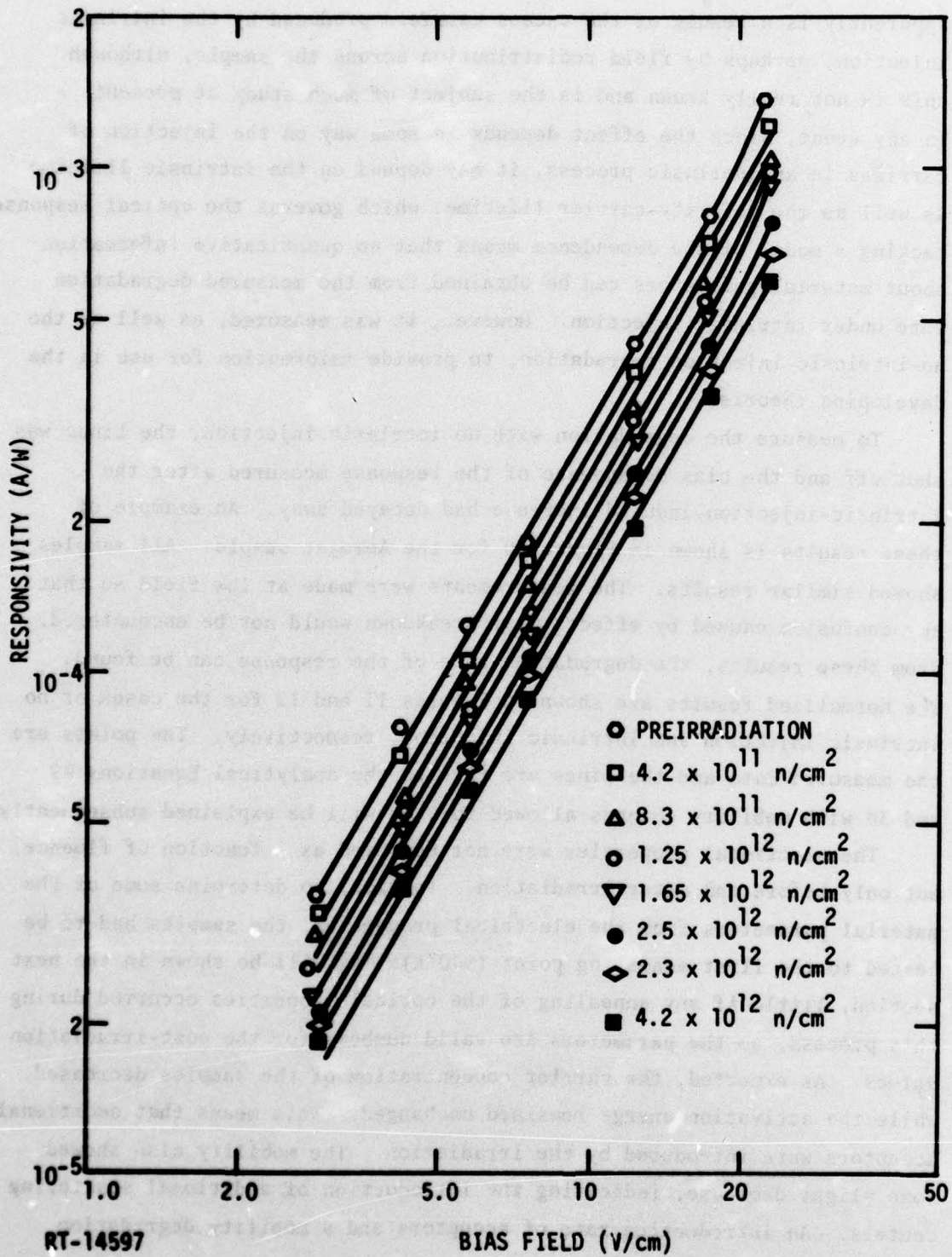


Figure 10. Responsivity degradation in the Aerojet sample

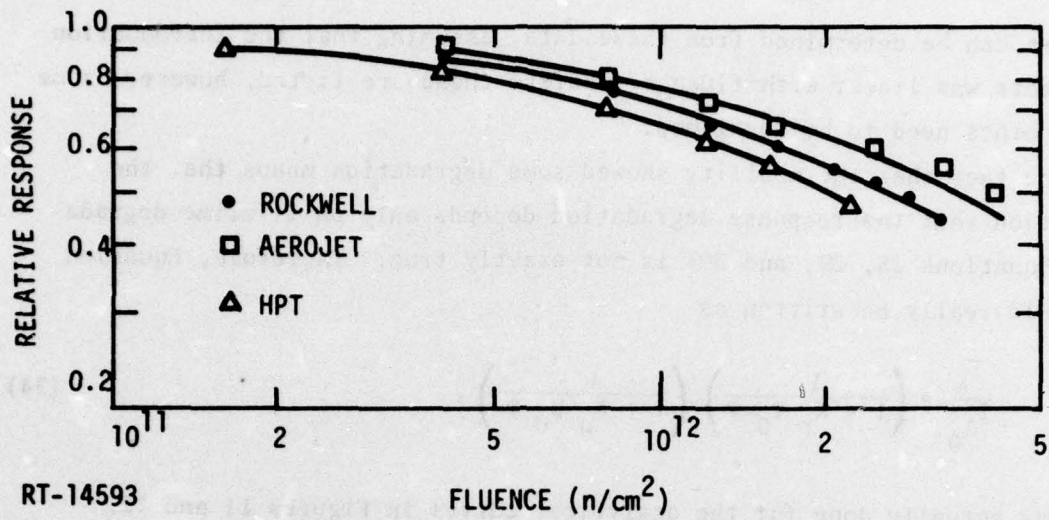


Figure 11. Response degradation in the Si:As samples with no intrinsic injection

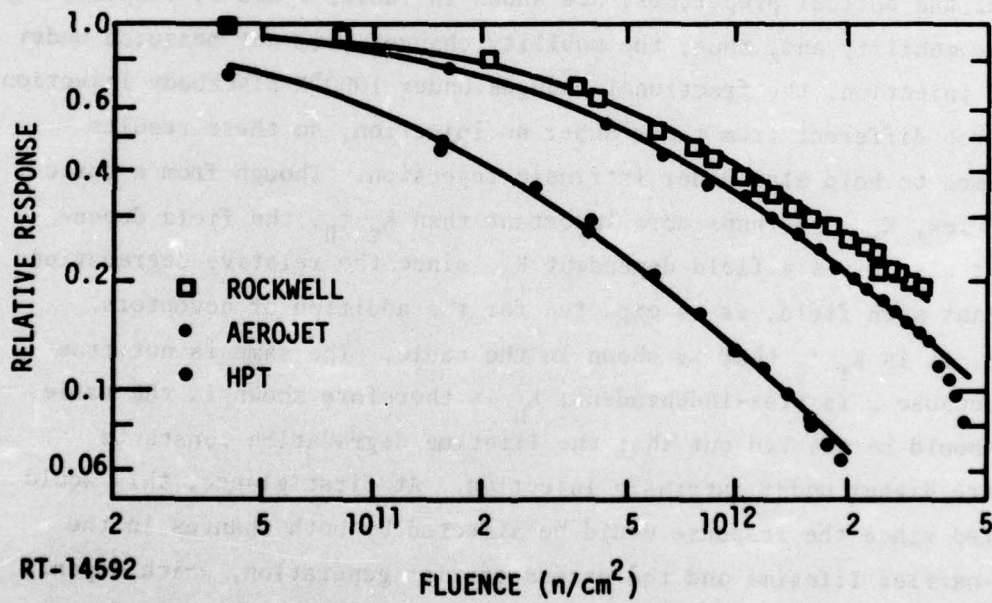


Figure 12. Response degradation in the Si:As samples with intrinsic injection

constant can be determined from these data, assuming that the introduction of defects was linear with fluence. Before these are listed, however, some other points need to be developed.

The fact that the mobility showed some degradation means that the assumption that the response degradation depends only on lifetime degradation (Equations 28, 29, and 30) is not exactly true. Therefore, Equation 29 should really be written as

$$\frac{I_{\lambda}}{I_{\lambda_0}} = \left(\frac{1}{1 + K_{\tau} \tau_0 \Phi} \right) \left(\frac{1}{1 + K_{\mu} \mu_0 \Phi} \right). \quad (34)$$

This was actually done for the analytical curves in Figures 11 and 12. Since it is the majority-carrier lifetime that is being considered, the acceptor introduction rate can be found from the response degradation using the electrically measured acceptor concentration. Conversely, the acceptor concentration can be found using the electrically measured introduction rate. The results of all these calculations, using the electrical and optical properties, are shown in Tables 4 and 5, respectively. Though the mobility and, thus, the mobility changes were not measured under intrinsic injection, the fractional changes under 1000°K blackbody injection were not too different from those under no injection, so these results were assumed to hold also under intrinsic injection. Though from a basic point of view, K_{τ} is perhaps more important than $K_{\tau} \tau_0$, the field dependence of τ also gives a field-dependent K_{τ} , since the relative degradation was constant with field, as is expected for the addition of acceptors. Therefore, it is $K_{\tau} \tau_0$ that is shown in the table. The same is not true for K_{μ} , because μ is bias-independent; K_{μ} is therefore shown in the table.

It should be pointed out that the lifetime degradation constants ($K_{\tau} \tau_0$) are higher under intrinsic injection. At first glance, this would be expected since the response would be affected by both changes in the majority-carrier lifetime and the excess-carrier generation, which depends on the intrinsic lifetime. Thus, both lifetimes should be reduced by irradiation. However it is actually the K_{τ} that is a measure of the rate

Table 4
 MATERIAL PARAMETERS OF Si:As SAMPLES FROM THE ELECTRICAL PROPERTIES MEASUREMENTS
 BEFORE AND AFTER IRRADIATION

Material Source	Preirradiation		Post Irradiation			
	N_a (cm^{-3})	μ ($\text{cm}^2/\text{V}\cdot\text{sec}$)	N_a (cm^{-3})	μ ($\text{cm}^2/\text{V}\cdot\text{sec}$)	$\frac{dN}{d\phi}$ (cm^{-1})	$K_t \tau_0$ ($\text{V}\cdot\text{sec}$)
Rockwell	5.3×10^{13}	2.45×10^4	9.8×10^{13}	2.1×10^4	13.7	2.1×10^{-18}
Aerojet	6.2×10^{13}	2.1×10^4	1.46×10^{14}	1.9×10^4	20.2	1.2×10^{-18}
HPT	5.2×10^{13}	4.1×10^4	8.7×10^{13}	3.5×10^4	15.6	2.1×10^{-18}

Table 5
 MATERIAL PARAMETERS OF Si:As SAMPLES FROM THE OPTICAL PROPERTIES MEASUREMENTS

Material Source	$K_t \tau_0$ (cm^2)	Assuming Measured N_a		$K_t \tau_0$ (cm^2)
		$\frac{dN}{d\phi}$ (cm^{-1})	N_a (cm^{-3})	
Rockwell	2.9×10^{-13}	15.4	4.7×10^{13}	1.25×10^{-12}
Aerojet	2.3×10^{-13}	14.3	8.8×10^{13}	1.8×10^{-12}
HPT	3.7×10^{-13}	19.3	4.2×10^{13}	5.7×10^{-12}

of change of the lifetime, so the different effective τ s must be allowed for. Because the response is higher at high intrinsic injection, the effective lifetime is higher. For the Rockwell and HPT samples, the ratio of the response under intrinsic injection to that under no intrinsic injection is almost equal to the ratio of the respective degradation constants. Further, this comparison is within a factor of two of being correct for the Aerojet material, and the discrepancy is in the direction where less degradation is observed than predicted by the lifetime difference. These results indicate that the same degradation process is occurring under both conditions and that intrinsic lifetime changes either do not occur or do not affect the response changes under intrinsic injection.

The comparison of the electrical and optical properties results is reasonable, considering the accuracy of the measurements. This is especially true of the electrical properties, where small changes in E_d have large effects on N_a . The largest discrepancy is for the Aerojet sample, and this is less than a factor of 1.5. Even this discrepancy is probably less as will be seen when the annealing is discussed.

Within the accuracy of the measurements, all of the acceptor introduction rates are equal. The average value is about 16 cm^{-1} . This is reasonable, because it is not expected that low-temperature damage in n-type silicon will depend on any impurity since the defects formed are thought to be immobile. The introduction rate of scattering centers (K_μ) is also probably the same for all materials within the experimental accuracy. The Aerojet sample, which had a lower measured constant, had a mobility change of less than 10% and even slight (5%) inaccuracies would put the number in agreement with that for the other two samples. Thus, the best value for K_μ is probably about $2 \times 10^{-18} \text{ V}\cdot\text{sec}$.

The electrical properties were measured before and after irradiation using the injection of the 1000°K blackbody to excite carriers. Thus, the carrier concentration is another measure of the lifetime, and it decreased as expected. However, since the effective lifetime depends on injection, and this is a steady-state measurement that cannot be directly

compared with the ac measurements of the photoconductivity, nothing more than the qualitative check is available here. The prime use of this measurement is in examining the annealing as discussed in the next section.

The final measurement that was performed was the spectral dependence of the response. The results are shown in Figure 13, with the normalization done to the preirradiation response so that changes are more readily observed. The scatter of the data was about $\pm 5\%$ in regions of atmospheric absorption and about twice as good elsewhere. The larger inaccuracy in regions of atmospheric absorption is because the measurement was single beam and the amounts of water vapor and CO_2 in the air varied from measurement to measurement.

Each sample showed a slightly different behavior. The Aerojet sample showed a definite rise in the response at wavelengths shorter than $3 \mu\text{m}$ on top of an essentially wavelength-independent degradation at all wavelengths. The HPT sample showed a short-wavelength rise, but to a much less extent than did the Aerojet sample. It also showed a degradation at all wavelengths, but this was not quite wavelength-independent and increased with increasing wavelength beyond $3 \mu\text{m}$. The Rockwell sample showed essentially a wavelength-independent degradation and perhaps a slight hint of a rise at short wavelengths. This rise would not be believable were it not for the fact that a rise was noted in the other two samples.

The rise at short wavelengths is gradual, with no well-defined step that would be the result of a defect with a fixed energy level. Instead, the shape of the gradual rise is similar to the near-edge absorption or band tailing observed in several prior studies of silicon irradiated at room temperature (Refs. 34,65,94,95). This band tailing appears to be the result of irradiation-induced disorder, which creates a continuum of states near the band edges and, thus, makes the "intrinsic" absorption band shift to longer wavelengths.

The difference in the extent of the band tailing in the different samples is qualitatively explained by the fluence received and the sample thickness. The Aerojet material received the highest fluence and also

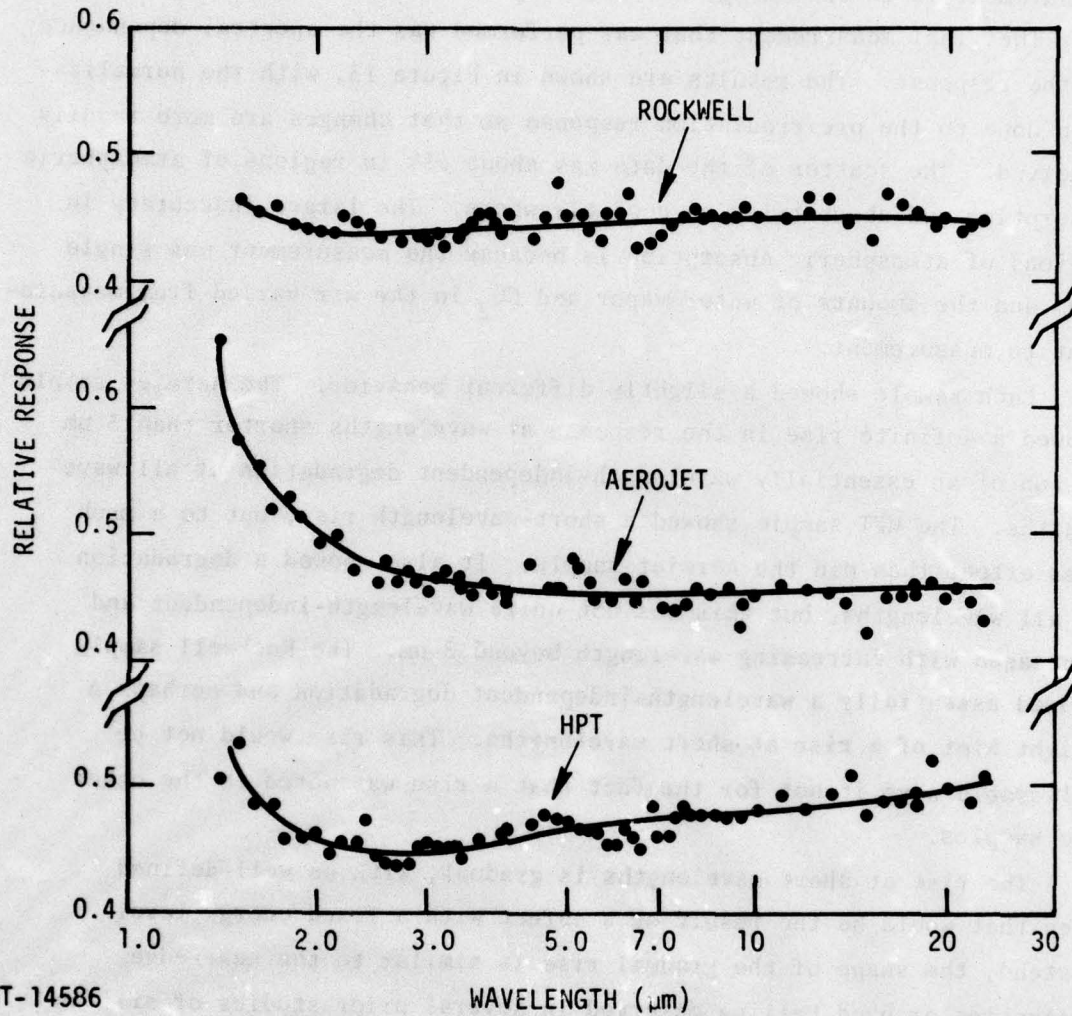


Figure 13. Post-irradiation spectral dependence of the response of the Si:As samples (normalized to the preirradiation response)

was the thickest, so it has a greater amount of damage and thus a larger band tailing. This qualitative argument predicts more band tailing for the Rockwell sample than for the HPT sample because their thicknesses were similar, and the former received a higher fluence. However, the fact that the opposite ordering was observed is not too troublesome, because band tailing in neither was very large and the measurement inaccuracies could easily have reversed the order. The inaccuracies exist particularly at the short wavelength end, where these effects are observed and where the impurity photoconductivity gives a very low response.

What the spectral dependence results clearly show is that, except for the band tailing, no defect photoconductivity was observed, and the primary effect of the irradiation was to lower the impurity response essentially uniformly at all wavelengths. This is the result of the decrease in majority carrier lifetime produced by the introduction of acceptor centers.

There are two other points concerning the spectral dependence measurements which must be discussed. The first concerns the general rise in response with increasing wavelengths of the HPT material. Though the cause is not understood, it possibly is related to the effect that caused the preirradiation response of this same sample to drop below that of the other two samples at short wavelengths.

The final point is the hint of an absorption band at $15 \mu\text{m}$ in all the samples. This band is quite small and is at the location of CO_2 absorption, which may well have produced the apparent band. This is another point that will be returned to in the discussion of the annealing.

EFFECTS OF ANNEALING

The isochronal annealing of the properties of the various samples was measured. Some discussion of the qualitative changes that occurred is necessary before the details of the annealing are examined. One feature that was observed was that the short-wavelength response degraded with respect to the long-wavelength response. Usually, this actually appeared to be an enhancement at long-wavelengths, as illustrated in

Figure 14. However, it sometimes appeared to be a depression at short wavelengths, as shown in Figure 15. To distinguish between the enhancement and depression and also to show the changes in the band tailing, the ratios of the response at a shorter wavelength (1.6 μm) and a longer wavelength (20 μm) to the response at an intermediate wavelength (4 μm) were used to examine annealing.

Another feature of the annealing which appeared in some instances was a change in the character of the carrier concentration versus inverse temperature curves. The prime example of this was the Rockwell sample following the 300, 330, and 365°K anneals. These results are shown in Figure 16. The slope of the curve seemed to become shallower at low temperature. This could indicate that shallow levels, perhaps as a result of disorder, were produced in sufficient numbers that they were not completely compensated at low temperatures.

The annealing results on the various samples are shown in Figures 17, 18, and 19. Annealing above 300°K was not performed on the HPT sample because of time constraints at the end of the program. The ordinate value is the ratio of the property value following annealing at the specified temperature to the preirradiation value of the property. The response was measured at both 4.1 μm and with the Al-on-Si filter, and both results are shown. The acceptor concentration results are actually the ratio of the preirradiation concentration to that after annealing, so that recovery is an increase towards 1.0, the same as for the response. The carrier concentration under intrinsic injection is another measure of the photoconductive response. Data for this property are not shown for the Rockwell sample because an equilibration time was necessary after the start of injection and this was not realized in this early experiment; the results, therefore, varied depending on the time used for the measurement. The mobilities with no intrinsic injection and under intrinsic injection were measured, except for the Rockwell sample, and both are shown. The spectral-dependence results are examined using the response ratios as explained previously. The long-wavelengths ratio is not shown for the Aerojet sample because it remained 1.0 throughout. The excess

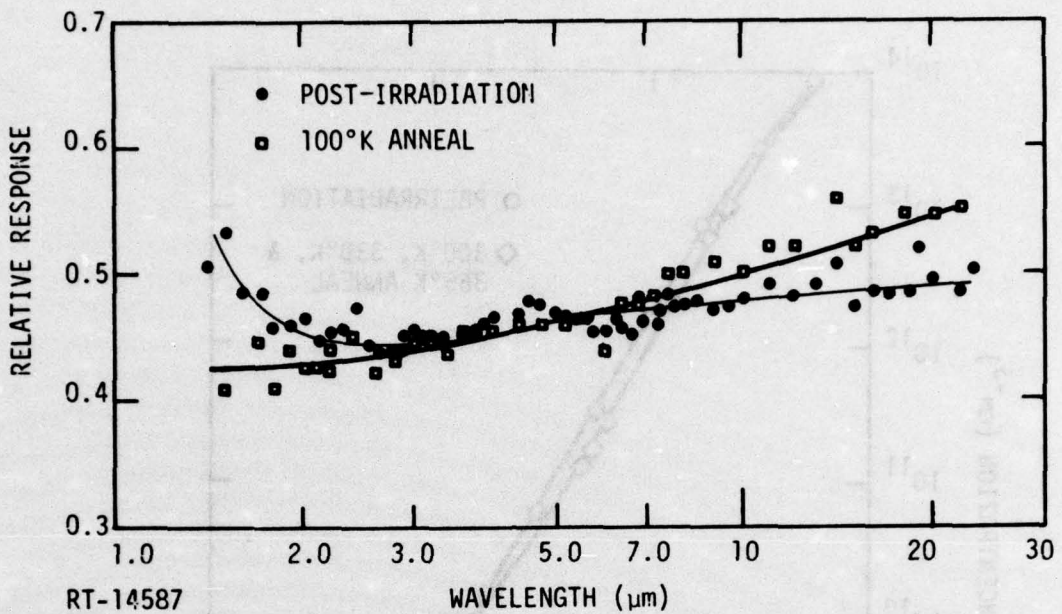


Figure 14. 100°K anneal of the Aerojet sample showing the long-wavelength enhancement of the response

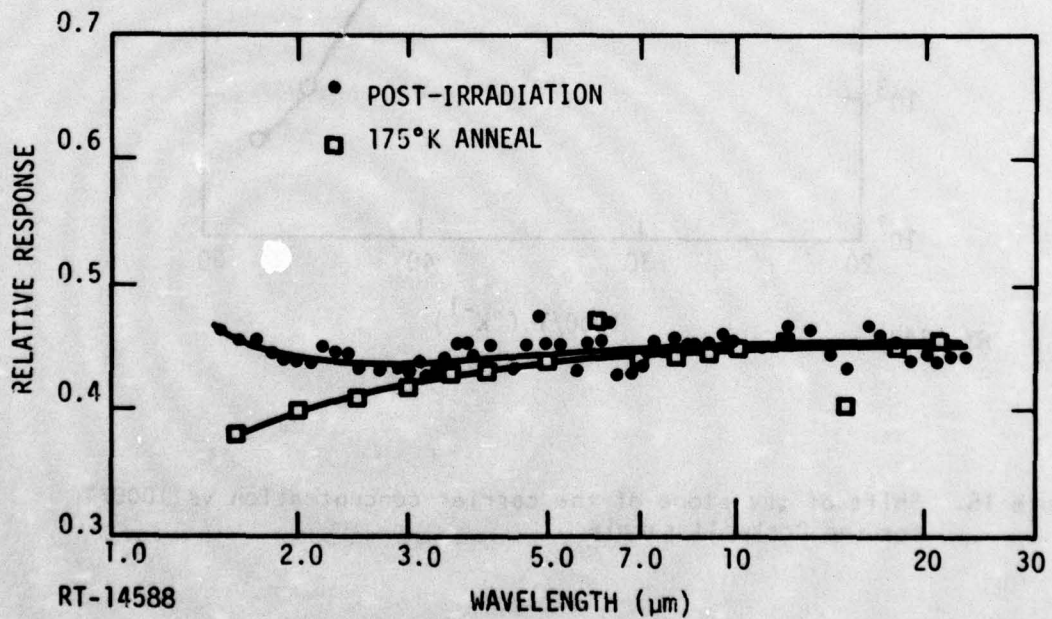


Figure 15. 175°K anneal of the Autonetics sample showing the short-wavelength depression of the response

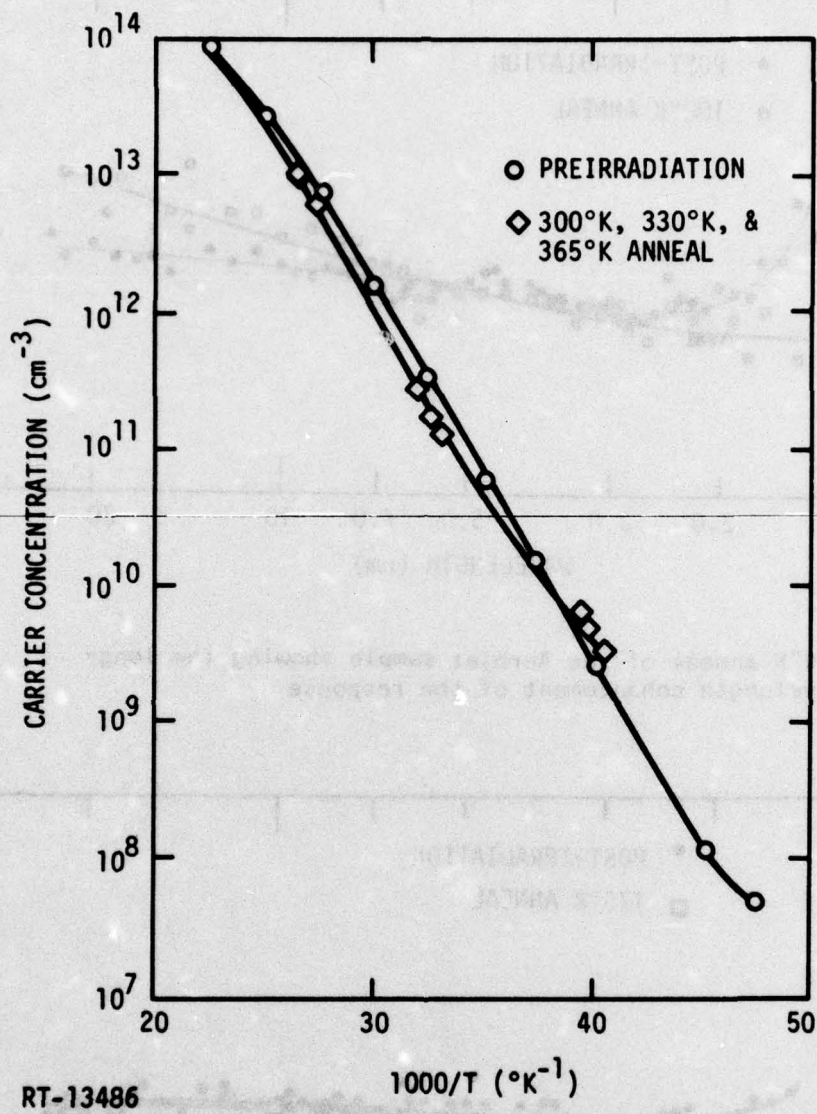


Figure 16. Shift of the slope of the carrier concentration vs 1000/T for the Rockwell sample

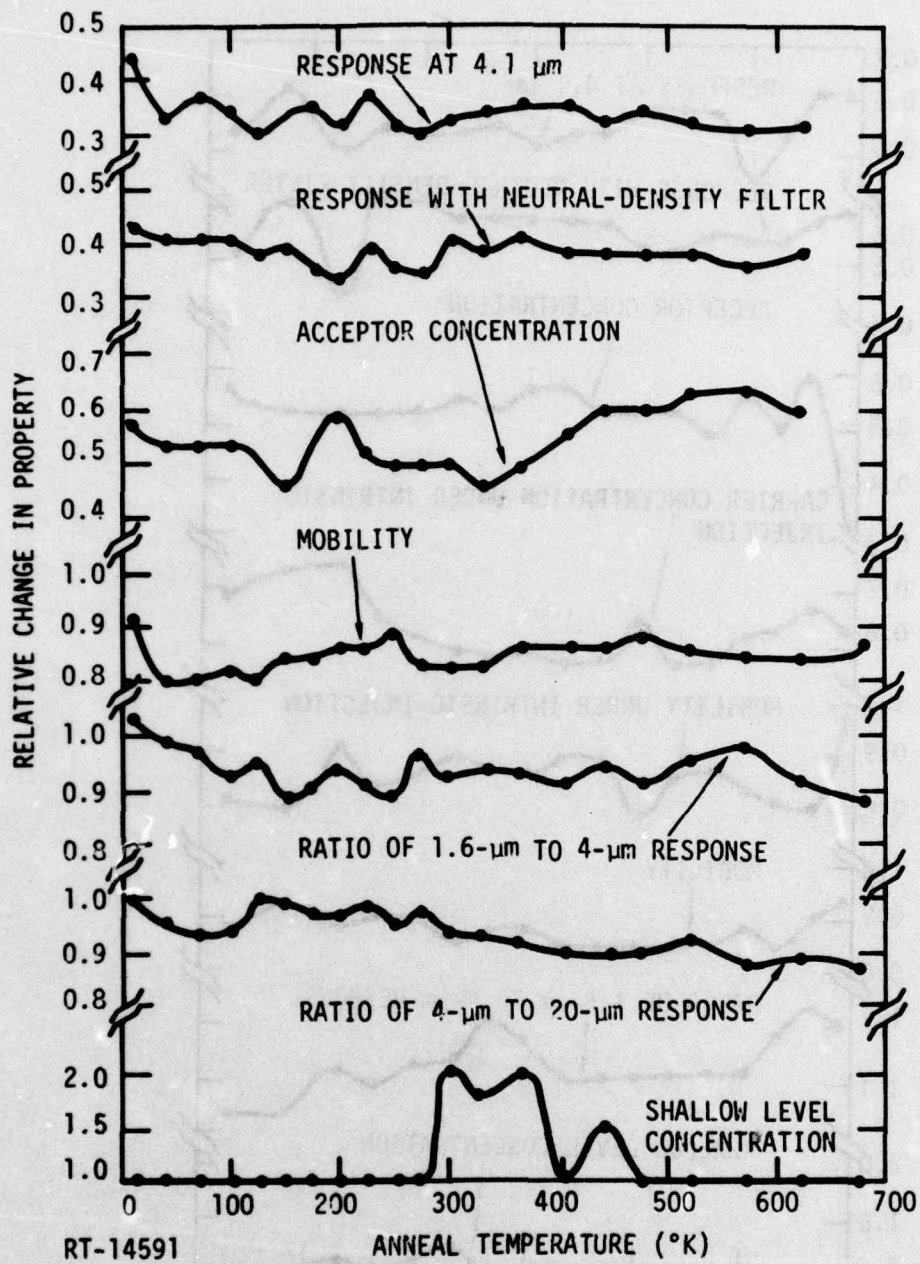


Figure 17. Annealing of the Rockwell sample

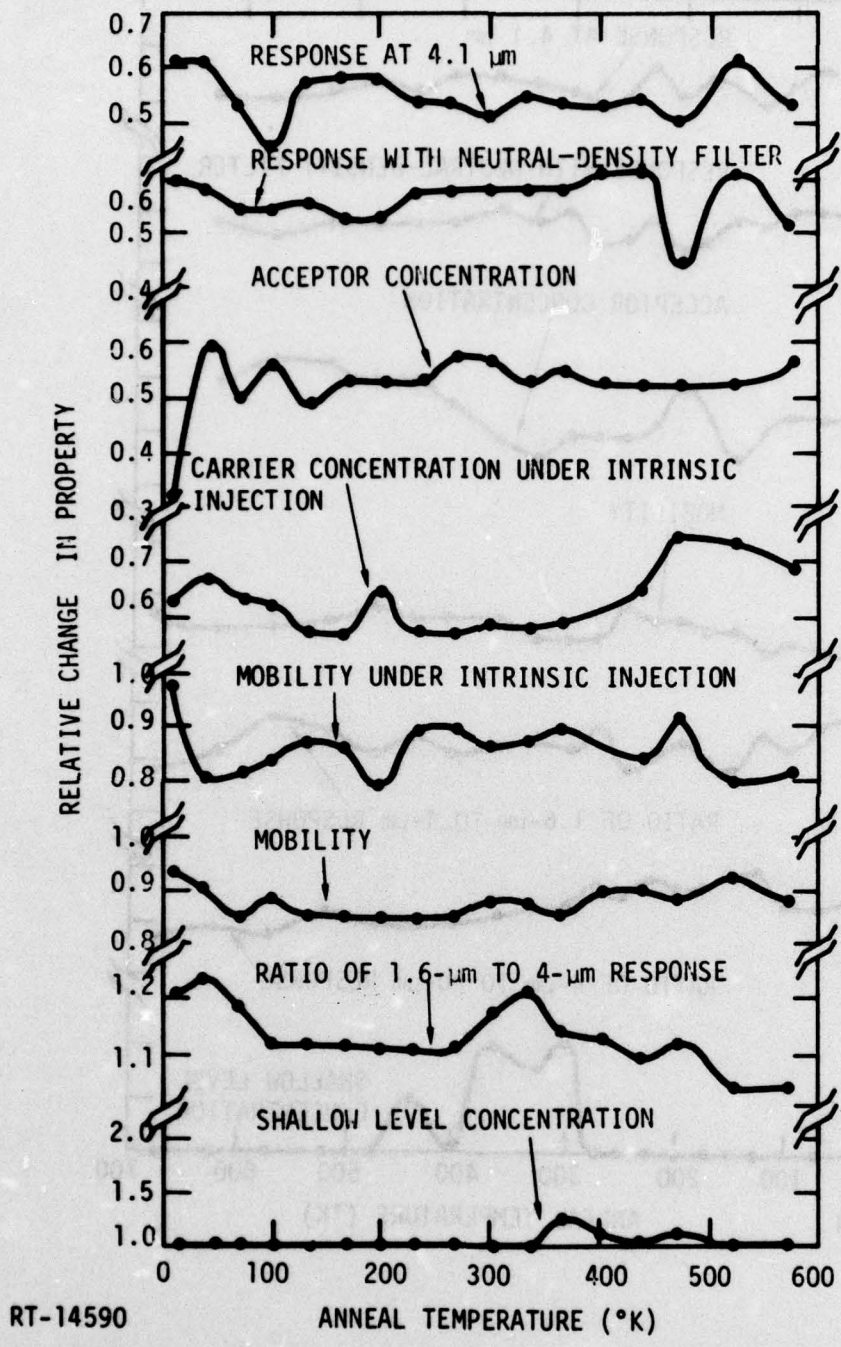
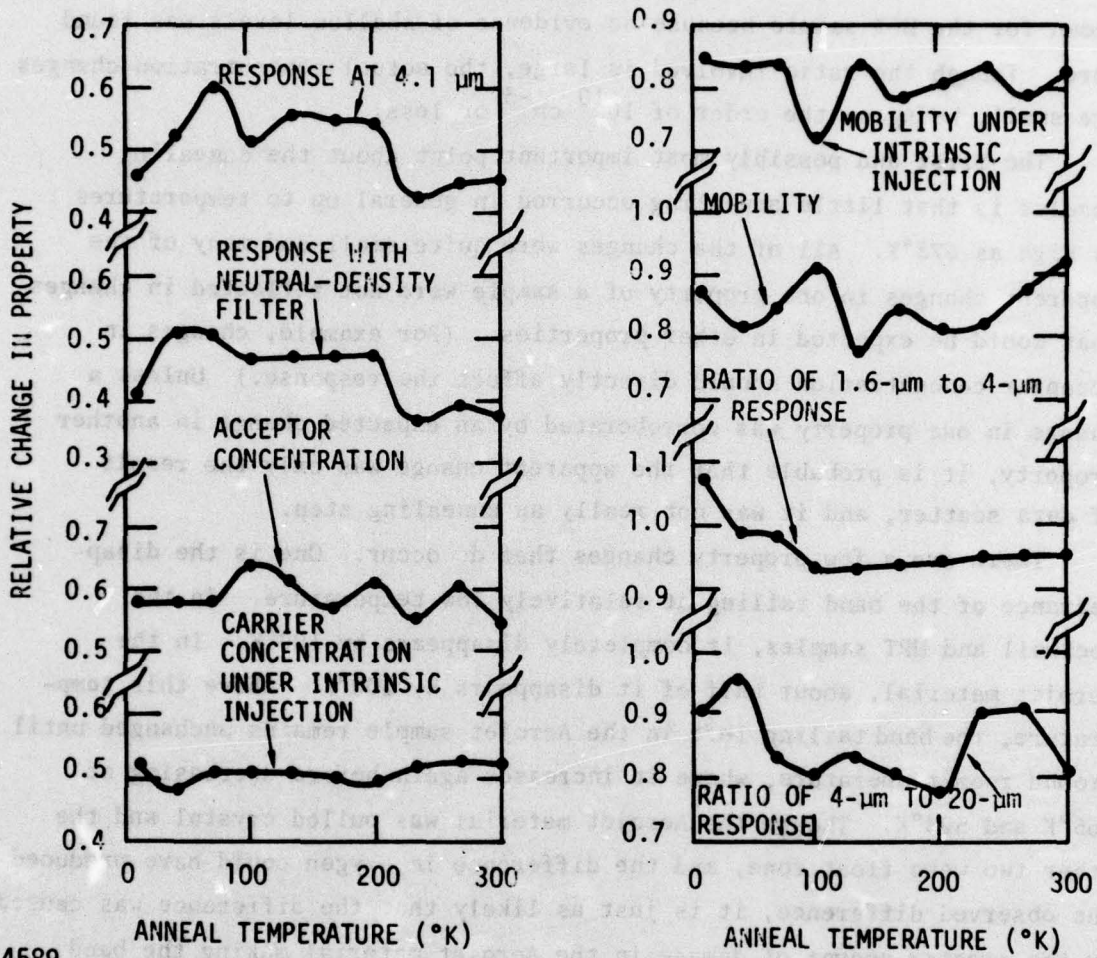


Figure 18. Annealing of the Aerojet sample



RT-14589

Figure 19. Annealing of the HPT sample

concentration of shallow levels is the ratio of the carrier concentration at low temperature to that of the line with the activation energy of the arsenic level extrapolated to the same temperature. This quantity is not shown for the HPT sample because no evidence of shallow levels was found here. Though the ratio involved is large, the actual concentration changes are small, being on the order of 10^{10} cm^{-3} or less.

The first and possibly most important point about the annealing results is that little annealing occurred in general up to temperatures as high as 673°K. All of the changes were quite small and many of the apparent changes in one property of a sample were not reflected in changes that would be expected in other properties. (For example, changes in acceptor concentration should directly affect the response.) Unless a change in one property was corroborated by an expected change in another property, it is probable that the apparent change was only the result of data scatter, and it was not really an annealing step.

There are a few property changes that do occur. One is the disappearance of the band tailing at relatively low temperature. In the Rockwell and HPT samples, it completely disappears by 100°K. In the Aerojet material, about half of it disappears by 100°K. Above this temperature, the band tailing left in the Aerojet sample remains unchanged until around room temperature, where it increases again before decreasing at 365°K and 523°K. Though the Aerojet material was pulled crystal and the other two were float zone, and the difference in oxygen could have produced the observed difference, it is just as likely that the difference was caused by the greater amount of damage in the Aerojet material making the band tailing easier to observe.

The 1.6- to 4- μm response ratio drops below 1.0 for the Rockwell and HPT samples. This is a result of the enhanced response at long wavelength (or decreased response at short wavelength) noted in these two samples. This shift in response gradually increases with increasing annealing temperature, though the increase is not monotonic and reverses occur at some temperatures. The reason the Aerojet sample does not show this effect is not understood. It is possible that the band tailing

present in this sample hid a short-wavelength depression. Or perhaps the amount of damage present changes the observed effect from an enhancement (band tailing) to a depression. In any event, this whole area is obviously not well understood.

In the Aerojet material, the acceptor concentration showed a large decrease, with 40°K annealing. Since this was not reflected in other properties of the sample and the other samples showed no similar decrease, it is likely that the post-irradiation measurement was falsely large. This was perhaps caused by trapping or some nonequilibrium condition. This would explain why the acceptor introduction rate in this sample as measured by the electrical properties was high compared to that measured by the optical properties or to that measured in the other samples. Assuming a nonequilibrium condition existed after irradiation, and the acceptor concentration after higher temperature annealing was actually the post-irradiation values, the introduction rate would be changed from 20.2 cm^{-1} , as listed in Table 4, to something on the order of 13 cm^{-1} , which would be in good agreement with the other numbers.

Other than this discounted acceptor concentration anneal in the Aerojet material, the only acceptor concentration change that may have been real was the slight recovery above room temperature in the Rockwell material. While the Aerojet sample showed no comparable recovery, the difference could well be caused by the oxygen concentration differences. The higher oxygen concentration in the Aerojet material could stabilize the damage. The optical response of the Rockwell material did not show any accompanying recovery. This could be because the acceptor concentration changes were only slight, or perhaps because this apparent annealing was not real.

The apparent addition of shallow levels in both the Rockwell and Aerojet samples occurred from about 300°K up to about 500°K, with the Aerojet sample shifted to somewhat higher temperature than the Rockwell one. There were slight apparent changes that occurred in the mobility and the short-wavelength region of the response that could have been connected with these shallow levels. All the changes, including those

in the carrier concentration, were small, and it is only the temperature coincidence of a number of changes that makes the annealing step more believable. The strange thing, however, is that larger mobility and short-wavelength response effects were observed at lower temperatures without shallow levels being observed in the carrier concentration. It may be that the damage present at low temperature does cause band changes which affect the short-wavelength photoconductivity which could be changed by across-the-band excitation, but must undergo rearrangement before it is in a form to produce shallow levels which communicate electrically with the conduction band. The HPT sample did not show the shallow level addition, probably because it was only annealed to 300°K, essentially below where the effects occur.

The mobility of all the samples showed only small changes with annealing, and probably none except perhaps those associated with the shallow-level changes were real. Thus, the irradiation-induced mobility changes were not affected by annealing.

The optical response of all the samples also showed only small changes with annealing, many of which were probably not real, though a few probably were. A reverse annealing step was observed at 233°K in the HPT sample, and a corresponding small step in the acceptor concentration as well as a step in the long-wavelength response ratio were also observed. Thus, a change probably did occur at this temperature in this sample. Strangely, neither of the other two samples showed anything that was definitely annealing at that temperature. The Aerojet sample showed some relatively large response changes at temperatures above 450°K that were probably real. The mobility and near-edge absorption showed small changes at the same temperatures which lends credibility to the fact that changes did occur.

In the end, the main result is that little annealing occurred and the damage introduced at 10°K was remarkably stable with temperature. If it were desired to examine the annealing more carefully, a larger amount of damage would have to be introduced so that the annealing changes would be large enough to be definitely observed above the scatter present in the data.

INTERPRETATION OF RESULTS

The most important effect produced by neutron irradiation of silicon at 10°K is the net introduction of acceptors. This introduction occurs at a rate of about 16 cm^{-1} and is apparently independent of oxygen concentration in the material, since it was about the same in both float-zone and pulled-crystal material. Though it would be expected that this introduction rate would also be independent of impurity type (at least for n-type material) and concentration, this conclusion cannot be reached from the results of this study, since all samples were arsenic doped and the concentrations varied by less than a factor of two. Further, the acceptor concentrations were also nearly identical, so no acceptor concentration dependence of the damage rate can be deduced either.

The increase in acceptor concentration results in more compensated donor (arsenic) sites. This produces a decrease in the carrier concentration at low temperatures, where it is governed by the acceptor concentration and, more importantly, a decrease in the majority-carrier lifetime because the additional empty arsenic sites give a higher concentration of sites into which optically excited carriers can drop. The decreased majority-carrier lifetime causes the optical response to degrade, and this is the effect of primary importance in the LWIR detector area. The response decrease is essentially uniform across the region of impurity photoconductivity, though some deviation to be discussed shortly does occur. There is no evidence of photoconductivity resulting from isolated defect levels. This is not surprising, because the defect concentration introduced in these tests was still orders of magnitude below the donor concentration, and the defects would need an extremely high cross section for interaction with the light to compete with the impurity photoconductivity.

Some evidence of the production of disorder is present in the appearance of a small amount of band tailing after irradiation. This could

be the result of the production of states near the band edges and the effective shift to lower energy of the band gap. This band tailing is temperature-unstable, and some or all of it annealed out in all samples by 100°K. When it disappeared, its place was taken by the long-wavelength enhancement (or short-wavelength depression) of the response. It is possible that this is also related to disorder. The short-wavelength depression could be produced by competitive absorption which does not result in photoconductivity. For example, the shallow states near the band edges may not readily communicate with the band, and thus the carriers excited to them across the gap have a low mobility. The long-wavelength enhancement could be produced by photoexcitation out of the shallow levels themselves. Apparently, the band tailing and the enhancement cannot exist at the same time because the Aerojet sample always showed band tailing but never any enhancement.

Band tailing was certainly observed in the irradiated samples. Though the extent of the band tailing was greater in the oxygen-containing (Aerojet) sample than in the others, the larger fluence and sample thickness of the former could easily explain the difference. Therefore, it is likely that, as expected, the production of band tailing is independent of oxygen concentration in the material. To be sure of this, a more detailed study of the band tailing would have to be performed. Rather than examining the photoconductivity alone, a better means of doing this would be to study the infrared absorption as well. Infrared absorption does not differentiate between photoconductivity-producing absorption and competitive absorption that depresses the photoconductivity. However, it is a more accurate technique for measuring effects near the band edge because the impurity photoconductivity is low in this region, but the transmission is high. Further, the use of a double beam technique such as absorption always results in improved accuracy.

The lack of stability of the band tailing is also odd, because room-temperature experiments (Refs. 33,34) had shown band tailing measured by photoconductivity techniques. However, the room-temperature experiments used relatively heavily-damaged material, and the most heavily

damaged of the samples studied here (the Aerojet sample) had some band tailing which remained after room temperature (and above) annealing. Thus, it appears that the damage concentration affects the stability of the band tailing in some manner. It may mean that a higher damage concentration results in the damage itself being more stable or that it produces more interaction between defects, which is what causes the band tailing. The latter explanation could also be supported by the presence of short-wavelength depression after the band tailing disappears. It could be that absorption occurs in both cases, but photoconductivity is produced only when there is sufficient interaction between defects to allow the electrons to move from defect to defect. Assuming that the defects involved (probably clusters) are introduced at about the same rate as acceptor centers (an unsupported assumption made so that order of magnitude estimates can be made), a defect concentration on the order of approximately 10^{14} cm^{-3} is required to see band tailing in the photoconductivity. For the interaction distance of one defect to overlap that of another defect, it would have to extend a few hundred lattice spacings. This, in fact, is on the order of the size of cluster regions (Ref. 51), which is some indirect evidence that the assumptions may be reasonable.

Even if the above assumptions about the band tailing and disorder are correct, the type of damage producing the most important effects is still unknown. That is, what the nature of the irradiation-induced acceptors is cannot be determined. They do not seem to be directly related to the band tailing, because no acceptor-related changes occur when the band tailing anneals. However, there is no indication of whether the acceptors are inside or outside of any cluster regions. To examine the nature of the acceptor centers, higher fluence irradiations to produce larger defect concentrations would be very useful. This would make the measured properties more dominated by the defects and less by the arsenic levels. Measurements using other experimental techniques might produce additional information about the defects.

There remains a question about the existence of shallow levels in the irradiated material. There were indications in the electrical properties data following some of the anneals of the existence of a low

concentration of shallow levels in the samples. Further, the short-wavelength depression and long-wavelength enhancement in the spectral response data may be caused by shallow levels. However, this connection is conjecture, which cannot be used to prove the existence of shallow-levels. The changes in the electrical properties and in the spectral response that may be the result of shallow levels were slight, and the annealing of the effects did not correlate with each other. To better study shallow levels, heavier irradiations to produce higher defect concentrations would have to be used.

The mobility showed a relatively small decrease following irradiation. Since the number of acceptors, and thus charged impurities, was approximately doubled by the irradiation, this means that the preirradiation mobility was not set principally by charged impurity scattering or the mobility would also have been changed a factor of two by irradiation. In fact, this reasoning implies that the preirradiation scattering is set more than 80% by other than charged-impurity scattering, probably by neutral-impurity scattering. This assumes that all charged sites are the measured acceptors and the corresponding compensated donors. This is a reasonable assumption, since the only other charged sites would be donors shallower than the arsenics, and few if any of these are observed in the photoconductivity. It also assumes that the irradiation-induced sites scatter as effectively as the preirradiation ones. This is also reasonable as a minimum, because the only significant change would occur if the sites had a different amount of charge, and higher charge on the irradiation-induced sites would result in more scattering from fewer sites and thus a higher estimate for neutral scattering in the unirradiated material.

One surprising thing about the damage is its temperature stability. Despite the fact that significant defect annealing, including cluster annealing, occurs in silicon below 300°K, very little change was noted in most of the irradiation-induced effects. What is possibly occurring is that the annealing actually involves defect rearrangement or evolution rather than disappearance and the new defects affect the measured

parameters in much the same way as the old ones. Thus, only those effects which are actually a direct effect of a certain defect (for example, band tailing) are observed to change with annealing. If this is true, larger defect concentrations, so that the defects are more dominant and direct defect effects (e.g., photoconductivity levels) can be observed, would be needed to study the annealing processes.

Some comments concerning the possible existence of a 15- μm absorption band are in order. The observed band was relatively small and exists in the same location as an atmospheric absorption band. Single-beam measurements such as photoconductivity, are potentially inaccurate in regions of atmospheric absorption. Therefore, the existence of the 15- μm band is certainly questionable, and the proof would have to come from a double-beam infrared absorption experiment.

The most important detector-related finding of this study is the degradation constant of the responsivity. The acceptor introduction rate was found to be about 16 cm^{-1} . Though the question of the dependence of this rate on donor or acceptor concentration remains, if the assumption of impurity independence is made, the responsivity degradation will follow

$$\frac{R}{R_0} = \frac{1}{1 + \frac{16\phi}{N_a}}$$

This assumption may be valid from a basic mechanisms point of view, but detectors with different concentrations of optical levels have been found to degrade at different rates. Whether this is caused by different acceptor concentrations (N_a) or a dependence of the introduction rate on impurity concentration is unknown. It is an important question and needs to be answered. The detector degradation will be essentially wavelength-independent and will be quite temperature stable. Thus, there is apparently no hardening procedure involving heating a damaged detector that exists.

CONCLUSIONS AND RECOMMENDATIONS

This section briefly lists the principle conclusions and recommendations of this study. The conclusions and the areas where further work is indicated are discussed in greater detail in previous sections.

The main effect of neutron irradiation at 10°K in arsenic-doped silicon is the introduction of acceptors at a rate of about 16 cm^{-1} . This causes the optical response and the low-temperature carrier concentration to decrease. This would be the most important cause of optical response degradation, because the mobility changes are much less. The introduction rate was found to be independent of oxygen concentration, but the dependence on arsenic or acceptor concentration was not determined. This dependence on arsenic or acceptor concentration is an important point and should be examined, because the maximum neutron fluence that detectors can survive depends on it.

The nature of the irradiation-induced defects which act as acceptors was not determined because they were only observed indirectly by their effect on the properties set by the impurities. To examine the nature of the defects, a higher defect concentration would be required so that direct effects of the defects could be observed. This could be an important point to study because, if the nature of the defects is understood, it might be possible to develop techniques to ameliorate their effects and thus to harden detectors.

The damage introduced was quite stable to annealing. This does not mean that the defects themselves are stable, because the defects were not observed and defect evolution could result in the same effect on the measured properties. Again, the way to examine defect annealing would be to introduce more defects so they could be observed directly.

There was some direct evidence of the production of disorder in the observance of band tailing in the photoconductivity following irradiation.

The band tailing was temperature-unstable, and significant annealing occurred by 100°K. There were indications that the effect is more stable at higher defect concentrations, perhaps because overlap of cluster regions is required for its observance. When the band tailing disappeared, a short wavelength depression of the response was noted. This may have been caused by the same absorption process without the production of photoconductivity. There was also some evidence to indicate the existence of shallow levels in the electrical properties measurements, but the number involved was quite small. To better study the production of disorder, infrared absorption measurements, which would more accurately examine band tailing, and larger defect concentrations should be used.

The irradiation-induced changes in the mobility were slight. Since the charged-impurity concentration increased by a much larger amount, this implies that the preirradiation mobility is dominated by neutral impurity scattering.

REFERENCES

1. L. J. Cheng and M. L. Swanson, Journal of Applied Physics **41**, 2627 (1970).
2. H. J. Stein, Applied Physics Letters **15**, 61 (1969).
3. V. S. Vavilov and A. F. Plotnikov, Journal of the Physical Society of Japan **18 Suppl. III**, 230 (1962).
4. C. D. Clark et al., Philosophical Magazine **20**, 301 (1969).
5. K. L. Starostin et al., Soviet Physics--Semiconductors **1**, 1520 (1968).
6. K. L. Starostin et al., Soviet Physics--Semiconductors **2**, 505 (1968).
7. K. L. Starostin, Soviet Physics--Semiconductors **4**, 1569 (1971).
8. H. J. Stein, Physical Review **163**, 801 (1967).
9. H. J. Stein, IEEE Transactions on Nuclear Science **NS-15**, 69 (1968).
10. F. L. Vook and H. J. Stein, Radiation Effects in Semiconductors, p. 99, New York: Plenum Press (1968).
11. V. N. Alfas'ev et al., Soviet Physics--Semiconductors **5**, 1967 (1971).
12. C. E. Barnes, IEEE Transactions on Nuclear Science **NS-16**, 28 (1969).
13. H. T. Henderson and K. L. Ashley, Physical Review **186**, 811 (1969).
14. C. E. Barnes, Radiation Effects **8**, 221 (1971).
15. M. Cherki and A. H. Kalma, IEEE Transactions on Nuclear Science **NS-16**, 24 (1969).
16. M. Cherki and A. H. Kalma, Physical Review B **1**, 647 (1970).
17. P. Vajda and L. H. Cheng, Radiation Effects **8**, 245 (1971).
18. K. L. Brower, Physical Review B **1**, 1908 (1970).
19. B. Goldstein, Radiation Effects **8**, 229 (1971).
20. G. D. Watkins et al., Journal of Applied Physics **30**, 1198 (1959).
21. G. D. Watkins, Journal of the Physical Society of Japan **18 Suppl. II**, 22 (1963).
22. G. D. Watkins, Radiation Damage in Semiconductors, p. 97, Dunod (1965).
23. G. D. Watkins, Symposium on Radiation Effects in Semiconductor Components, p. A1-9, *Journées d'Electronique* (1968).
24. G. D. Watkins, Radiation Effects in Semiconductors, p. 97, New York: Plenum Press (1968).
25. G. D. Watkins, IEEE Transactions on Nuclear Science **NS-16**, 13 (1969).
26. P. S. Gwozdz and J. S. Koehler, Physical Review B **6**, 4571 (1973).

27. E. E. Klontz and L. L. Sivo, Radiation Effects in Semiconductors, p. 136, New York: Plenum Press (1968).
28. R. E. McKeighen and J. S. Koehler, Radiation Effects 9, 59 (1971).
29. F. L. Vook, Physical Review 138, A1234 (1965).
30. L. H. Cheng, Physics Letters 24A, 729 (1967).
31. L. H. Cheng, Radiation Effects in Semiconductors, p. 143, New York: Plenum Press (1968).
32. M. Caillot et al., Physica Status Solidi A 4, 121 (1971).
33. A. H. Kalma and J. C. Corelli, Radiation Effects in Semiconductors, p. 153, New York: Plenum Press (1968).
34. A. H. Kalma and J. C. Corelli, Physical Review 173, 734 (1968).
35. B. Goldstein et al., Colloque International sur les Cellules Solaires, Toulouse (1970).
36. M. Cherki and A. H. Kalma, Proceedings of the Third Intl. Conr. on Photoconductivity, p. 279, Pergamon Press (1971).
37. I. P. Akimchenko et al., Soviet Physics--Semiconductors 3, 132 (1969).
38. I. P. Akimchenko et al., Soviet Physics--Solid State 10, 3677 (1964).
39. V. D. Tkachev et al., Soviet Physics--Solid State 5, 1332 (1964).
40. V. D. Tkachev et al., Soviet Physics--Solid State 5, 2333 (1964).
41. E. Fenimore et al., Journal of Applied Physics 43, 1962 (1972).
42. R. C. Young and J. C. Corelli, Physical Review B 5, 1455 (1972).
43. M. T. Lappo and V. D. Tkachev, Soviet Physics--Semiconductors 4, 1882 (1970).
44. P. F. Lugakov and V. D. Tkachev, Soviet Physics--Semiconductors 1, 295 (1967).
45. P. F. Lugakov and V. D. Tkachev, Soviet Physics--Semiconductors 1, 569 (1967).
46. V. D. Tkachev and M. T. Lappo, Radiation Effects 9, 81 (1971).
47. V. S. Vavilov et al., Soviet Physics--Solid State 4, 2522 (1965).
48. A. B. Gerasimov et al., Soviet Physics--Solid State 8, 2390 (1967).
49. M. L. Swanson, Physica Status Solidi 33, 721 (1969).
50. M. Bertolotti et al., Journal of Applied Physics 38, 2645 (1967).
51. M. Bertolotti, Radiation Effects in Semiconductors, p. 311, New York: Plenum Press (1968).
52. J. M. Pankratz et al., Journal of Applied Physics 39, 101 (1968).
53. J. M. Pankratz and N. L. Rudee, Physica Status Solidi 26, K97 (1968).

54. K. L. Brower, Radiation Effects **8**, 123 (1971).
55. K. L. Brower, Physical Review B **4**, 1968 (1971).
56. D. F. Daly and H. E. Nofke, Radiation Effects **8**, 203 (1971).
57. D. F. Daly and H. E. Nofke, Radiation Effects **10**, 191 (1971).
58. W. Jung and G. S. Newell, Physical Review **132**, 648 (1963).
59. Y-H Lee and J. W. Corbett, Physical Review B **9**, 4351 (1974).
60. Y-H Lee and J. W. Corbett, Physical Review B **8**, 2810 (1973).
61. C. S. Chen and J. C. Corelli, Radiation Effects **9**, 75 (1971).
62. C. S. Chen and J. C. Corelli, Physical Review B **3**, 1505 (1972).
63. L. J. Cheng and P. Vajda, Journal of Applied Physics **40**, 4679 (1969).
64. L. J. Cheng and P. Vajda, Physical Review **186**, 816 (1969).
65. L. H. Cheng and J. Lori, Physical Review **171**, 859 (1968).
66. L. J. Cheng and J. Lori, Applied Physics Letters **16**, 324 (1970).
67. J. C. Corelli et al., IEEE Transactions on Nuclear Science **NS-17**, 128 (1970).
68. T. D. Dzhaferov, Soviet Physics--Semiconductors **5**, 697 (1971).
69. Yu. P. Koval' et al., Soviet Physics--Semiconductors **5**, 2061 (1972).
70. E. N. Lotkova, Soviet Physics--Solid State **6**, 1224 (1964).
71. A. K. Ramdas and M. G. Rao, Physical Review **142**, 451 (1966).
72. F. L. Vook and H. J. Stein, Radiation Effects **2**, 23 (1969).
73. R. E. Whan, Journal of Applied Physics **37**, 3378 (1966).
74. J. A. Neber et al., Radiation Effects **8**, 239 (1971).
75. V. N. Mordkovich et al., Soviet Physics--Semiconductors **6**, 1643 (1973).
76. I. Arimura, IEEE Transactions on Nuclear Science **NS-17**, 348 (1970).
77. O. L. Curtis, Jr., IEEE Transactions on Nuclear Science **NS-17**, 105 (1970).
78. B. L. Gregory and H. H. Sander, Proceedings of the IEEE **58**, 1328 (1970).
79. J. W. Harrity and C. E. Mallon, IEEE Transactions on Nuclear Science **NS-17**, 100 (1970).
80. R. E. Leadon, IEEE Transactions on Nuclear Science **NS-17**, 110 (1970).
- 80a. C. E. Mallon and J. W. Harrity, IEEE Transactions on Nuclear Science **NS-18**, 45 (1971).
81. J. R. Srour and O. L. Curtis Jr., Journal of Applied Physics **40**, 4082 (1969).

82. J. A. Naber and A. H. Kalma, 10th Midcourse Measurements Meeting, 251 (1971).
83. J. A. Naber and A. H. Kalma, Nuclear Effects on Optics Seminar (1971).
84. J. A. Naber and A. H. Kalma, Nuclear Effects on Optics Technical Briefing, 1.7.1 (1972).
85. A. H. Kalma and B. C. Passenheim, Nuclear Effects on Optics Technical Briefing, 3.3.1 (1972).
86. A. H. Kalma et al., Proceedings on IRIS 18, No. 2, 137 (1973).
87. A. H. Kalma et al., Joint Strategic Sciences Meeting (1974).
88. A. H. Kalma et al., "Detector Radiation Damage Effects Vol. IV," report number MS-ABMDA-1697 (May 1973).
89. A. H. Kalma et al., "Detector Radiation Damage Effects Study, Vol. III," report number DNC74EG566581 (July 1974).
90. A. H. Kalma, "Hardened Detector/Circuit Development, Vol. III," report number 5059 (September 1974).
91. M. Warren, "Investigation of Nuclear Radiation Effects on Infrared Detectors" report number AFCRL-TR-73-0346 (August 1973).
92. R. A. Florence, "Hardened Focal Plane Development", Vol. I Appendix A, "Permanent Damage Nuclear Effects Study", A. H. Kalma, report number DASG-75-C-0044 (August 1974).
93. A. H. Kalma, "Hardened Detectors/Circuits Study, Vol. III", report number 5254 (October 1976).
94. L. J. Cheng et al., Physical Review 152, 761 (1966).
95. A. H. Kalma, IEEE Transactions on Nuclear Science NS-20, 224 (1973).
96. A. H. Kalma, et al., Journal of Applied Physics 37, 3913 (1966).
97. See for example: J. S. Blakemore, "Semiconductor Statistics," Pergamon Press, (1962).